Supporting Information for:

Acid-Base Responsive Switching Between "3+1" and "2+2" Platinum Complexes

Dhassida Sooksawat, [a] *Sarah J. Pike,* [a] *Alexandra M. Z. Slawin,* [b] *Paul J. Lusby** [a]

[a] EaStCHEM School of Chemistry, University of Edinburgh, The King's Buildings, West Mains Road, Edinburgh, EH9 3JJ, UK

[b] EaStCHEM School of Chemistry, University of St. Andrews, Purdie Building, St. Andrews, Fife, KY16 9ST, UK

E-mail: Paul.Lusby@ed.ac.uk

General Experimental Information

Unless stated otherwise, all reagents and solvents were purchased from commercial sources and used without further purification. $H_2\mathbf{L^1}$,[1] [$\mathbf{L^1}$Pt(DMSO)],[2] [$\mathbf{L^1}$Pt(DMAP)],[3] [$\mathbf{L^1}$Pt(py)],[3] 1,1'-propane-2,2-diylbis[4-(4-bromobutoxy)benzene][4] and 2-phenylethylazide[5] were prepared according to literature procedures. All reactions, unless stated otherwise, were carried out under a nitrogen atmosphere. Column chromatography was carried out on silica using Kiesegel C69 (Merck, Germany) as the stationary phase and TLC was performed on precoated silica 60 gel plates (0.20 mm thick, $60F_{254}$. Merck, Germany) and observed under UV light. All ^{1}H NMR and ^{13}C NMR spectra were recorded as stated on either a Bruker AV 500 or AV 400 instrument at a constant temperature of 298 K. Chemical shifts are reported in parts per million. Coupling constants (*J*) are reported in hertz (Hz) and are reported as observed. Where more than one *J* value is given per chemical shift, the first refers to coupling through three bonds, the second refers to coupling through four bonds, etc.. Standard abbreviations indicating multiplicity were used as follows: m = multiplet, d = doublet, dd = doublet of doublet, s = singlet, t = triplet, td = triplet of doublet, br = broad. The presence of ^{195}Pt satellites is indicated by a subscripted satellite following the multiplicity abbreviation (the magnitude of this splitting is indicated using ^{3}J (^{195}Pt-H), for a typical 3-bond coupling to platinum). Other abbreviations used in the Supporting Information, include; DMAP = 4-dimethylaminopyridine; DMF = dimethylformamide; DMSO = dimethylsulfoxide; EDTA = ethylenediamine tetraacetic acid; 3,5-lut = 3,5-lutidine; P_1-^{t}Bu = tert-butylaminotris(dimethylamino)phosphazene; py = pyridine, rt = room temperature; TBAF = tetrabutylammonium fluoride; TCE = 1,1,2,2-tetrachloroethane; THF = tetrahydrofuran; TLC = thin layer chromatography; TsOH = *p*-toluenesulfonic acid. All melting points (m.p.) were determined using Sanyo Gallenkamp apparatus. FAB and ESI mass spectrometry was carried out by the services at the University of Edinburgh.

Synthetic Details and Characterisation Data

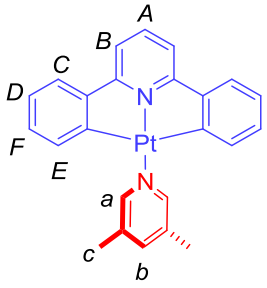

[**L**^{1}Pt(3,5-lut)]

To a yellow solution of [**L**^{1}Pt(DMSO)] (0.093 g, 0.19 mmol) in CH_2Cl_2 (10 mL) was added 3,5-lutidine (0.040 g, 0.37 mmol), which resulted in a darkening of the solution to orange. The reaction was stirred for 18 h at rt and the excess solvent was removed under reduced pressure. Purification of the crude product using column chromatography (1:1:0.01; CH_2Cl_2:hexane:NEt_3) gave the compound as an orange solid (0.052 g, 53 %). Bright orange crystals suitable for X-ray crystallography were grown *via* slow diffusion of diisopropyl ether into a saturated CH_2Cl_2 solution of the desired complex. m.p. 205-210 °C (dec.); ^{1}H NMR (500 MHz, CD_2Cl_2): 8.68 ($s_{satellite}$, ^3J (^{195}Pt-H) = 45.2 Hz, 2H, H_a), 7.56 (t, J = 8.0 Hz, 1H, H_A), 7.51 (s, 1H, H_b), 7.45 (dd, J = 7.6, 0.6 Hz, 2H, H_C), 7.29-7.24 (m, 2H, H_B), 7.20-7.14 (m, 2H, H_F), 7.07-7.01 (m, 2H, H_D), 6.95 – 6.87 (m, 2H, H_E), 2.39 (s, 6H, H_c); ^{13}C NMR (125 MHz, CD_2Cl_2): 173.1, 168.6, 151.4, 149.8, 139.9, 138.4, 136.4, 133.7, 130.9, 124.3, 123.9, 114.8, 18.5; LRESI-MS: *m/z* = 532 $[MH]^+$; HRESI-MS: *m/z* = 531.12649 $[M]^+$ (calc. for $C_{24}H_{20}N_2{}^{195}Pt$, 531.12687).

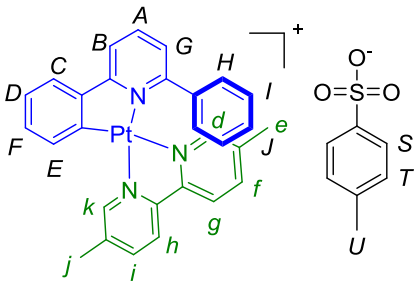

[H**L**^{1}Pt(dmbipy)]OTs

To a solution of [**L**^{1}Pt(DMSO)] (0.50 g, 10.0 mmol) in CH_2Cl_2 (30 mL) was added 5,5′-dimethyl-2,2′-bipyridyl.TsOH (0.37 g, 10.0 mmol) and the reaction mixture stirred at rt for 5 minutes. After this time, the solution was concentrated to ~ 3 mL under reduced pressure and upon the slow addition of hexane, the desired product precipitated from solution as a bright

yellow solid. The crude solid was filtered off and collected. Crystals suitable for X-ray crystallography were grown *via* slow diffusion of diisopropyl ether into a saturated chloroform solution (0.48 g, 78%). ^{1}H NMR (500 MHz, CD_2Cl_2); δ = 9.28 ($s_{satellite}$, ^{3}J (^{195}Pt-H) = 35.6 Hz, 1H, H_k), 8.46 (d, J = 8.2 Hz, 1H, H_h), 8.34 (br, 2H, H_H), 8.27 (d, J =8.2 Hz, 1H, H_g), 8.20-8.13 (m, 2H, H_{A+i}), 7.96 (d, J = 8.0 Hz, 1H, H_G), 7.77-7.68 (m, 5H, $H_{B+J+f+S}$), 7.65 (s, 1H, H_d), 7.44 (d, J = 7.6 Hz, 1H, H_E), 7.34 (td, J = 7.6, 1.5 Hz, 1H, H_F), 7.32-7.19 (m, 4H, H_{D+C+I}), 7.11 (d, J = 8.0 Hz, 2H, H_T), 2.62 (s, 3H, H_j), 2.32 (s, 3H, H_U), 2.21 (s, 3H, H_e); ^{13}C NMR (125 MHz, CD_2Cl_2); 168.0, 160.5, 155.9, 152.8, 151.7, 148.8, 147.8, 145.8, 142.2, 141.8, 140.5, 140.4, 139.1, 138.8, 138.0, 136.9, 132.5, 131.5, 130.2, 129.8, 128.9, 128.5, 126.5, 125.7, 125.3, 125.0, 124.7, 123.4, 118.6, 21.5, 19.4, 18.9; LRESI-MS: *m/z* = 611 $[M-OTs]^+$; HRESI-MS: *m/z* = 611.17716 (calc. for $C_{29}H_{26}N_3{}^{195}Pt$, 611.17690).

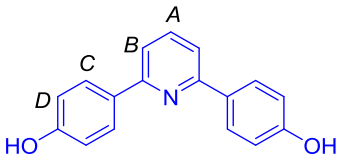

2,6-(bis-4-hydroxyphenyl)pyridine

Adapted from a procedure by Aucagne *et al*.[6] Isopropanol (50 mL) was purged with nitrogen for 5 minutes then potassium *tert*-butoxide (2.24 g, 20 mmol), PEPPSI-IPr (0.27 g, 5 mol%), 4-hydroxyphenylboronic acid (2.43 g, 17.6 mmol) and 2,6-dibromopyridine (1.89 g, 8 mmol) were added and the reaction flask was resealed and purged with nitrogen. The reaction mixture was stirred at rt for 48 h, then quenched with saturated NH_4Cl solution (100 mL) and extracted with EtOAc (3×100 mL). The combined organic layers were dried over $MgSO_4$, filtered, concentrated under reduced pressure, then purified by column chromatography (0-30% Et_2O in CH_2Cl_2) providing the desired product as a pale yellow solid (1.53 g, 73%). m.p. 222-226 °C; ^{1}H NMR (500 MHz, CD_3OD); 7.97 (d, J = 8.8 Hz, 4H, H_C), 7.77 (t, J = 7.8 Hz, 1H, H_A), 7.59 (d, J = 7.8 Hz, 2H, H_B), 6.90 (d, J = 8.8 Hz, 4H, H_D); ^{13}C NMR (125 MHz, CD_3OD); 160.0, 158.1, 138.8, 132.3, 129.4, 118.2, 116.4; LR-FABMS (3-NOBA matrix): *m/z* = 263 $[M]^+$; HR-FABMS (3-NOBA matrix); *m/z* = 263.09510 (calc. for $C_{17}H_{13}O_2N$, 263.09518).

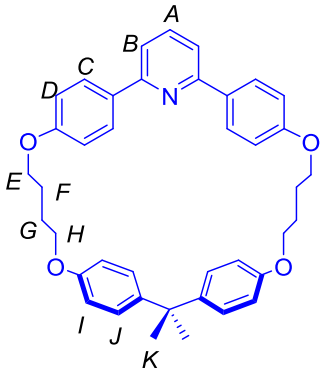

$H_2\mathbf{L}^2$

To a stirred mixture of Cs_2CO_3 (19.68 g, 60 mmol) and 2,6-(bis-4-hydroxyphenyl)pyridine (0.27 g, 1.0 mmol) in 600 mL of degassed DMF at 65 °C was added dropwise, using a pressure equalising funnel, over a period of 24 h a solution of 1,1′-propane-2,2-diylbis[4-(4-bromobutoxy)benzene] (0.51 g, 1.0 mmol) in 200 mL of degassed DMF. When addition was complete, the reaction was stirred at 65 °C for a further 30 h. After this time, the reaction mixture was cooled to rt, the solvent removed under reduced pressure, and the residue partitioned between CH_2Cl_2 and H_2O. The organic phase was separated, and the aqueous phase extracted twice with CH_2Cl_2. The combined organic phases were washed with brine, H_2O and dried over $MgSO_4$. The solvent was removed under reduced pressure and the residue purified by column chromatography (25-50% CH_2Cl_2:Petroleum ether) to give a colourless solid as the product (0.70 g, 80%) m.p. 203-206 °C; ^{1}H NMR (500 MHz, $CDCl_3$); 8.01 (d, J = 8.1 Hz, 4H, H_C), 7.73 (t, J = 7.4 Hz, 1H, H_A), 7.54 (d, J = 7.4 Hz, 2H, H_B), 7.16 (d, J = 8.1 Hz, 4H, H_J), 6.99 (d, J = 8.1 Hz, 4H, H_D), 6.82 (d, J = 8.1 Hz, 4H, H_I), 4.24 (t, J = 6.8 Hz, 4H, H_E), 4.01 (t, J = 5.7 Hz, 4H, H_H), 2.05-1.98 (m, 4H, H_F), 1.98-1.92 (m, 4H, H_G), 1.63 (s, 6H, H_K); ^{13}C NMR (125 MHz, $CDCl_3$); 159.5, 156.8, 156.5, 143.1, 137.4, 132.5, 128.4, 127.8, 117.0, 115.2, 113.8, 67.8, 67.3, 41.8, 31.3, 25.8, 25.5; LR-FABMS (3-NOBA matrix) m/z = 600 $[MH]^+$; HR-FABMS (3-NOBA matrix) m/z = 600.31179 (calc. for $C_{40}H_{42}NO_4$ 600.31084)

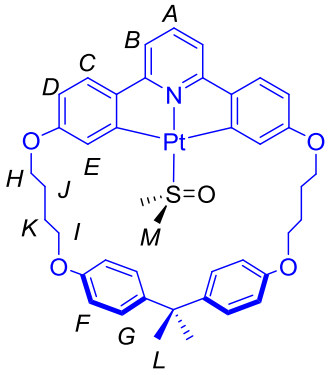

[$\mathbf{L}^2$Pt(DMSO)]

To a solution of $H_2\mathbf{L}^2$ (0.24 g, 0.40 mmol) in acetic acid (12 mL) was added $K_2[PtCl_4]$ (0.17 g, 0.40 mmol) and tetrabutylammonium chloride (0.13 g, 0.40 mmol). The mixture was heated at 125 °C for 2 days over which time the suspension turned green-yellow with some unconsumed red Pt salt. The entire solids were filtered off and then washed with water (5 mL) to remove the red starting Pt salt. The resultant green-yellow precipitate was washed with acetone (5 mL) and Et_2O (5 mL). The green-yellow solid was then dissolved in hot DMSO (6 mL) and K_2CO_3 (0.57 g, 4.1 mmol) and H_2O (2 mL) were added. The mixture was heated to 90 °C for 2 h. Upon the addition of more water (10 mL) the product precipitated as a bright yellow solid. Flash column chromatography (CH_2Cl_2) and crystallization from Et_2O and CH_2Cl_2 gave the product as a bright yellow solid. (0.28 g, 80%). m.p. >270 °C (dec.); ^{1}H NMR (500 MHz, $CDCl_3$); δ 7.48 (t, J = 8.0 Hz, 1H, H_A), 7.36 (d, J = 8.5 Hz, 2H, H_C), 7.34 (d, J = 2.5 Hz, 2H, H_E), 7.14 (d, J = 8.8 Hz, 4H, H_G), 7.05 (d, J = 8.0 Hz, 2H, H_B), 6.84 (d, J = 8.8 Hz, 4H, H_F), 6.58 (dd, J = 8.5, 2.5 Hz, 2H, H_D), 4.17 (t, J = 6.4 Hz, 4H, H_H), 4.07 (t, J = 6.2 Hz, 4H, H_I), 3.14 (s, 6H, ^3J (^{195}Pt-H) = 25.4 Hz, H_M), 2.02-1.90 (m, 8H, H_{J+K}), 1.62 (s, 6H, H_L); ^{13}C NMR (125 MHz, $CDCl_3$); δ 168.4, 166.5, 160.7, 157.1, 143.3, 142.5, 141.0, 127.8, 126.1, 121.5, 114.2, 113.2, 112.0, 68.01, 67.99, 48.0, 41.7, 31.1, 26.5, 26.0; LR-ESIMS m/z = 871 $[MH]^+$; HR-ESIMS m/z = 871.27380 (calc. for $C_{42}H_{46}NO_5{}^{195}Pt^{32}S$ 871.27391).

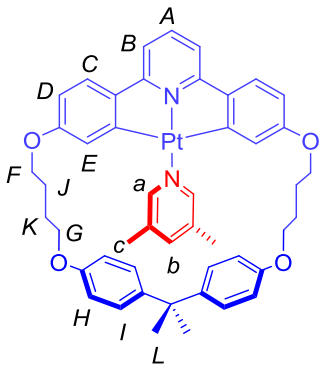

[$\mathbf{L}^2$Pt(3,5-lut)]

To a yellow solution of [$\mathbf{L}^2$Pt(DMSO)] (0.032 g, 0.037 mmol) in CH_2Cl_2 (5 mL) was added 3,5-lutidine (0.004 g, 0.037 mmol), which resulted in a darkening of the solution to orange. The reaction was stirred at 40 °C overnight and the excess solvent was removed under reduced pressure. The crude residue was purified by Et_2O diffusion into a saturated CH_2Cl_2 solution, yielding the product as bright orange crystals (0.012 g, 37%). ^{1}H NMR (500 MHz, CD_2Cl_2); δ 8.45 ($s_{satellite}$, 2H, ^3J (^{195}Pt-H) = 43.4 Hz, H_a), 7.43 (t, J = 8.0 Hz, 1H, H_A), 7.36 (d, J = 8.4 Hz, 2H, H_C), 7.18 (d, J = 8.7 Hz, 4H, H_I), 7.03 (d, J = 8.0 Hz, 2H, H_B), 6.72 (s, 1H, H_b), 6.65 (d, J = 8.7 Hz, 4H, H_H), 6.54 (dd, J = 8.4, 2.5 Hz, 2H, H_D), 6.41 ($d_{satellite}$, J = 2.5 Hz, 2H, ^3J (^{195}Pt-H) = 27.3 Hz, H_E), 3.98 (t, J = 6.5 Hz, 4H, H_F), 3.78 (t, J = 6.5 Hz, 4H, H_G), 1.88-1.78 (m, 14H, $H_{J,K,c}$), 1.67 (s, 6H, H_L); ^{13}C NMR (125 MHz, CD_2Cl_2); δ 175.3, 167.5, 160.8, 157.0, 150.7, 143.2, 141.8, 139.2, 137.9, 135.4, 127.5, 125.4, 117.2, 114.3, 112.4, 111.6, 67.9 ,67.4, 41.2, 29.9, 25.7, 25.4, 17.5; LR-FABMS (3-NOBA matrix) *m/z* = 900 $[MH]^+$; HR-FABMS (3-NOBA matrix) *m/z* = 900.33538 (calc. for $C_{47}H_{49}N_2O_4{}^{195}$Pt 900.33346).

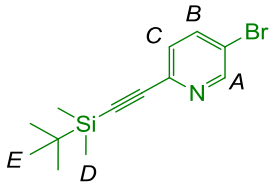

2-*tert*-butyldimethylsilylethynyl-5-bromopyridine

To a suspension of 5-bromo-2-iodopyridine (0.85 g, 3 mmol), CuI (0.06 g, 10 mol%), $Pd(PPh_3)_2Cl_2$ (0.10 g, 5 mol%) in dry THF (20 mL) and Et_3N (15 mL) at 0 °C was charged *tert*-butyldimethylsilylacetylene (0.58 mL, 3 mmol). The colour changed from yellow to dark brown. The reaction mixture was stirred at 0 °C for 1 h before being warmed to rt and then left stirring overnight. A white precipitate formed and the solution had turned yellow. The mixture was filtered through celite and washed with Et_2O. The filtrate was concentrated

under reduced pressure. The resulting residue was dissolved in CH_2Cl_2, washed with brine and dried over $MgSO_4$. Following filtration and removal of the solvent under reduced pressure, the residue was purified by column chromatography (0-50% CH_2Cl_2/hexane) to give a colourless solid (0.73 g, 82%). m.p. 89-92 °C; ^{1}H NMR (500 MHz, $CDCl_3$); δ 8.63 (d, J = 2.0 Hz, 1H, H_A), 7.77 (dd, J = 8.3, 2.4 Hz, 1H, H_B), 7.34 (dd, J = 8.3, 0.5 Hz, 1H, H_C), 1.00 (s, 9H, H_E), 0.20 (s, 6H, H_D); ^{13}C NMR (125 MHz, $CDCl_3$); 151.2, 141.6, 138.9, 128.6, 120.4, 103.5, 95.1, 26.3, 16.8, -4.7; LRESI-MS: m/z = 296 $[MH]^+$; HRESI-MS: m/z = 296.046565 (calc. for $C_{13}H_{19}NSiBr$ 296.04647)

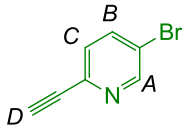

2-ethynyl-5-bromopyridine

To a solution of 2-*tert*-butyldimethylsilylethynyl-5-bromopyridine (0.15 g, 0.50 mmol) in CH_2Cl_2 (3 mL) was added TBAF (1M in THF, 0.5 mL, 0.50 mmol), which resulted in the colourless solution turning yellow. The solution was stirred at rt for 3 h and then the solvent was removed under reduced pressure. The residue was purified by column chromatography (0-50% CH_2Cl_2/hexane) to get the product as an off white solid (0.07 g, 78%). m.p. 80-83 °C; ^{1}H NMR (500 MHz, $CDCl_3$); δ 8.65 (d, J = 2.1 Hz, 1H, H_A), $_C$), 3.22 (s, 1H, H_D); ^{13}C NMR (125 MHz, $CDCl_3$); 151.3, 140.6, 138.9, 128.4, 120.8, 81.8, 78.5; LRESI-MS: m/z = 182 $[MH]^+$; HRESI-MS: m/z = 181.960374 (calc. for C_7H_5NBr 181.95999)

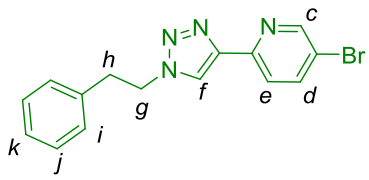

L^3

To a colourless solution of 2-ethynyl-5-bromopyridine (0.018 g, 0.10 mmol) and 2-phenylethylazide (0.025 g, 0.10 mmol) in TCE (10 mL) was added $Cu(CH_3CN)_4PF_6$ (0.042 g, 0.11 mmol). The resultant yellow solution was then stirred at rt for 1 h before being heated at 70 °C for 18 h. After cooling to rt, the mixture was filtered through celite and washed with TCE. The filtrate was concentrated under reduced pressure. The resulting residue was dissolved in CH_2Cl_2, washed with 0.1 M Sodium EDTA, dried over $MgSO_4$. The product

was obtained as a colourless solid following purification by from column chromatography (CH_2Cl_2) (0.018 g, 55%). ^{1}H NMR (500 MHz, $CDCl_3$); δ 8.60 (d, J = 2.2 Hz, 1H, H_c), 8.06 (d, J = 8.4 Hz, 1H, H_e), 7.92 (s, 1H, H_f), 7.89 (dd, J = 8.4, 2.2 Hz, 1H, H_d), 7.33-7.28 (m, 2H, H_j), 7.26-7.24 (m, 1H, H_k), 7.15 (d, J = 7.1 Hz, 2H, H_i), 4.65 (t, J = 7.4 Hz, 2H, H_g) 3.27 (t, J = 7.4 Hz, 2H, H_h); ^{13}C NMR (125 MHz, $CDCl_3$); δ 150.6, 148.8, 147.4, 139.7, 136.9, 129.1, 128.8, 127.4, 122.5, 121.5, 119.6, 52.0, 36.8; LR-FABMS (3-NOBA matrix) m/z = 329 $[MH]^+$; HR-FABMS (3-NOBA matrix) m/z = 329.03933 (calc. for $C_{15}H_{14}BrN_4$ 329.03964)

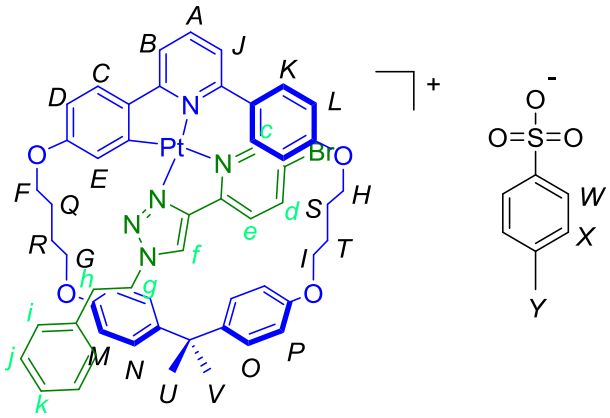

trans-[$\mathbf{L}^2$Pt($\mathbf{L}^3$)]OTs

To a yellow solution of [$\mathbf{L}^2$Pt(DMSO)] (0.012 g, 0.013 mmol) in CH_2Cl_2 (5 mL) was added $\mathbf{L}^3$ (0.004 g, 0.013 mmol) and TsOH (0.002 g, 0.013 mmol), which resulted in a changing of the solution to greenish yellow. The solution was stirred at rt for 1 h and the excess solvent was removed under reduced pressure. The yellow solid was recrystallized in CH_2Cl_2 and Et_2O (0.005 g, 34 %). For the ^{1}H-^{1}H NOESY assisted assignment of *trans*-[$\mathbf{L}^2$Pt($\mathbf{L}^3$)]OTs, see pages S42 and S43.^{1}H NMR (500 MHz, CD_2Cl_2); δ 9.94 (s, 1H, H_f), 8.29 (d, J = 8.4 Hz, 1H, H_e), 8.00 (t, J = 7. 8 Hz, 1H, H_A), 7.97 (d, J = 2.4 Hz, 1H, H_E), 7.95 (ddd, J = 8.4, 2.1, 0.9, 1H, H_d), 7.88 (d, J = 1.9 Hz, 1H, H_c), 7.71 (d, J = 7.9 Hz, 2H, H_W), 7.67 (d, J = 8.0 Hz, 1H, H_B), 7.57-7.52 (m, 2H, H_{J+C}), 7.30-7.25 (m, 2H, H_j), 7.24-7.16 (m, 3H, H_{k+i}), 7.14-7.07 (m, 4H, $H_{X+N/O}$), 7.04 (d, J = 8.2 Hz, 2H, $H_{O/N}$), 6.80 (dd, J = 8.5, 2.4, 1H, H_D), 6.75-6.69 (m, 4H, H_{M+P}), 4.61-4.53 (m, 1H, $H_{g'}$), 4.52-4.43 (m, 1H, $H_{g''}$), 4.42-4.34 (m, 1H, $H_{F'}$), 4.19-4.04 (m, 3H, $H_{F''+G}$), 4.04-3.89 (m, 4H, H_{H+I}), 3.28 (m, 2H, H_h), 2.31 (s, 3H, H_Y), 2.20-1.93 (m, 5H, $H_{Q+R+S'}$), 1.92-1.82 (m, 1H, $H_{S''}$), 1.82-1.70 (m, 2H, H_T), 1.60 (s, 3H, $H_{U/V}$), 1.57 (s, 3H, $H_{V/U}$); ^{13}C NMR (125 MHz, CD_2Cl_2); δ 168.0, 161.2, 159.8, 159.3, 157.4, 157.3, 150.0, 149.9, 146.1, 143.8, 143.5, 142.8, 140.0, 139.6, 139.2, 136.8, 130.4, 129.4, 129.3, 129.0, 128.6, 128.21, 128.19, 127.7, 126.4, 126.1, 123.7, 122.1, 120.6, 119.0, 116.8, 114.4, 114.3,

113.9, 68.3, 68.0, 67.95, 67.9, 53.7, 42.0, 36.2, 31.5, 30.3, 26.2, 26.0, 25.8, 25.5, 21.5; LR-FABMS (3-NOBA matrix) *m/z* = 1122 $[MH]^+$; HR-FABMS (3-NOBA matrix) *m/z* = 1122.30287 (calc. for $C_{55}H_{54}BrN_5O_4{}^{195}Pt$ 1122.30014).

Ligand Exchange Experiments

(i) Acyclic Cyclometallated Pt Complexes

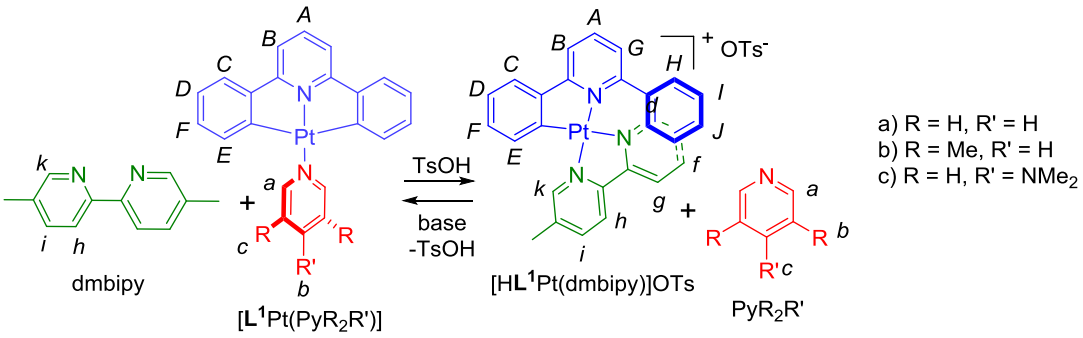

Scheme S1. Acid-Base responsive switching between "3+1" and "2+2" cyclometallated Pt complexes.

General procedure

To a solution of [**L**^{1}Pt(PyR$_2$R')] (4.0 μmol) in CD_2Cl_2 (0.30 mL) at 298 K was added dmbipy (4.0 μmol). The subsequent addition TsOH in 97:3 CD_2Cl_2:CD_3OD (5.2, 9.6 and 10.8 μmol of TsOH for the experiments with [**L**^{1}Pt(py)], [**L**^{1}Pt(3,5-lut)] and [**L**^{1}Pt(DMAP)], respectively), followed by agitation for 1 minute, caused the solution to lighten. A ^{1}H NMR spectrum was then recorded immediately, confirming quantitative conversion to [H**L**^{1}Pt(dmbipy)]OTs. P$_1$-^{t}Bu in CD_2Cl_2 (20 μmol) was added directly to the NMR tube and the solution agitated for one minute. ^{1}H NMR spectra were recorded at regular intervals until no further change was observed. The backward reaction of "2+2" to "3+1" complex was complete in 1.5 h for [**L**^{1}Pt(py)] and 2 h for [**L**^{1}Pt(3,5-lut)] and [**L**^{1}Pt(DMAP)].

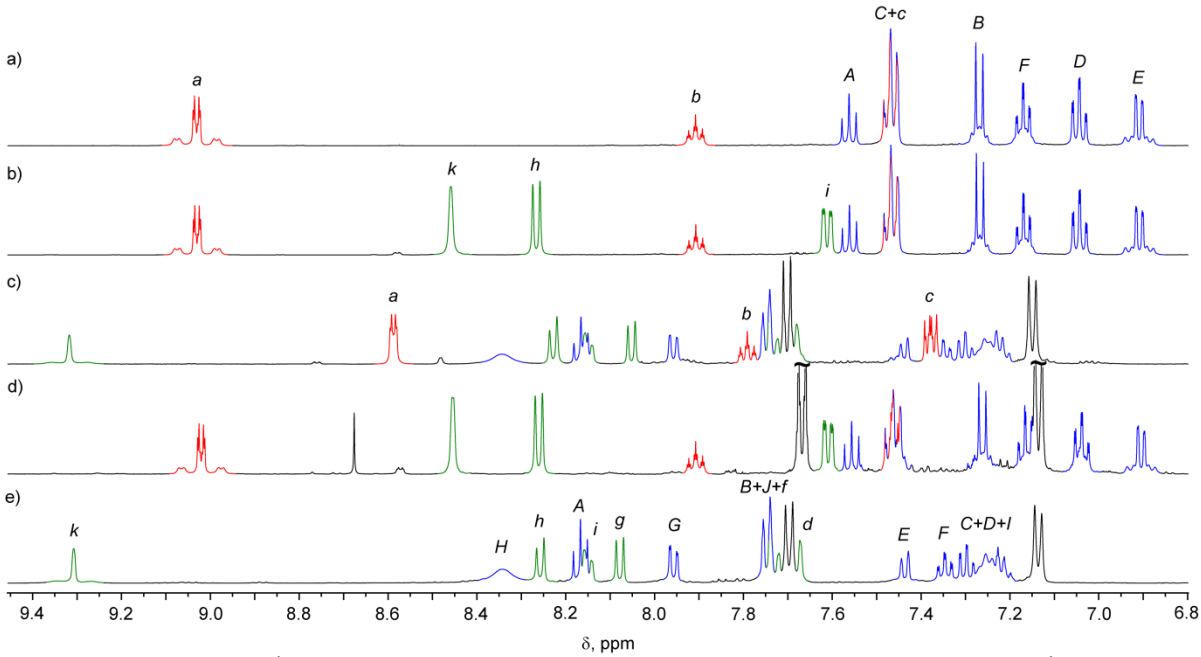

Figure S1. Partial ^{1}H NMR spectra (500 MHz, CD_2Cl_2, 298 K) of a) [**L**^{1}Pt(py)]; b) [**L**^{1}Pt(py)] + 5,5'-dimethyl-2,2'-bipyridine; c) [**L**^{1}Pt(py)] + 5,5'-dimethyl-2,2'-bipyridine, 5 minutes after the addition of 1.3 eq. TsOH; d) 1.5 h after the subsequent addition of 5 eq. P_1-^{t}Bu; e) Authentic [H**L**^{1}Pt(dmbipy)]OTs (containing 3% CD_3OD). The assignments correspond to the lettering shown in Scheme S1 (page S10).

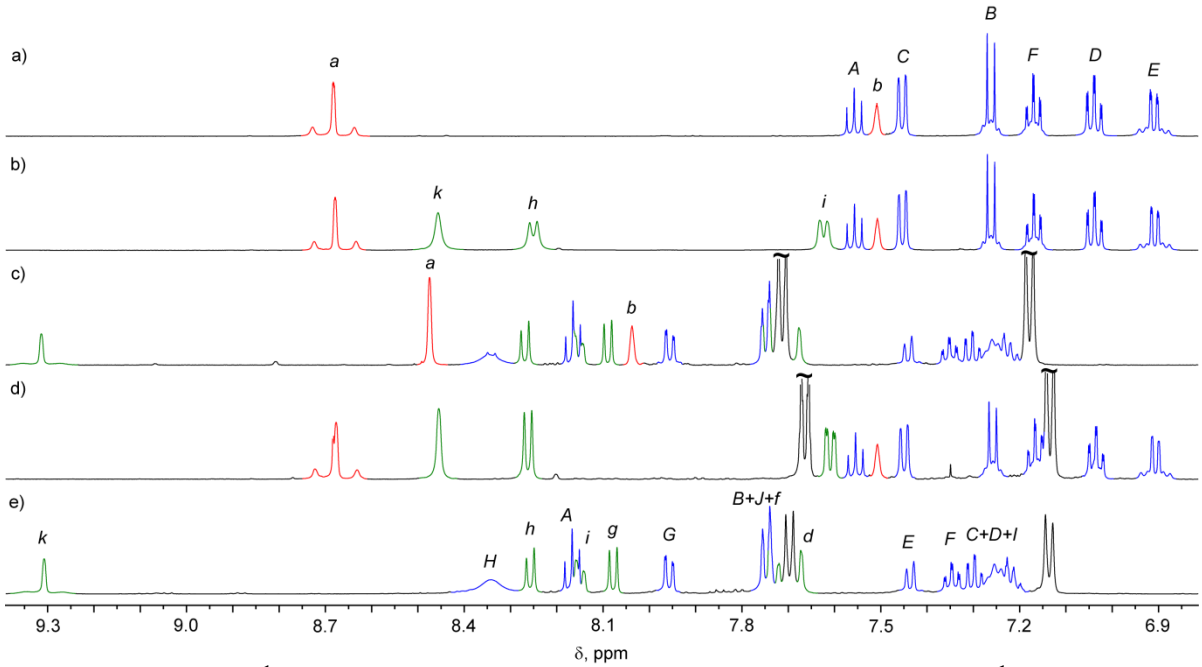

Figure S2. Partial ^{1}H NMR spectra (500 MHz, CD_2Cl_2, 298 K) of a) [**L**^{1}Pt(3,5-lut)]; b) [**L**^{1}Pt(3,5-lut)] + 5,5'-dimethyl-2,2'-bipyridine; c) [**L**^{1}Pt(3,5-lut)] + 5,5'-dimethyl-2,2'-bipyridine, 5 minutes after the addition of 2.4 eq. TsOH; d) 2 h after the subsequent addition of 5 eq. P_1-^{t}Bu; e) Authentic [H**L**^{1}Pt(dmbipy)]OTs (containing 3% CD_3OD). The assignments correspond to the lettering shown in Scheme S1 (page S10).

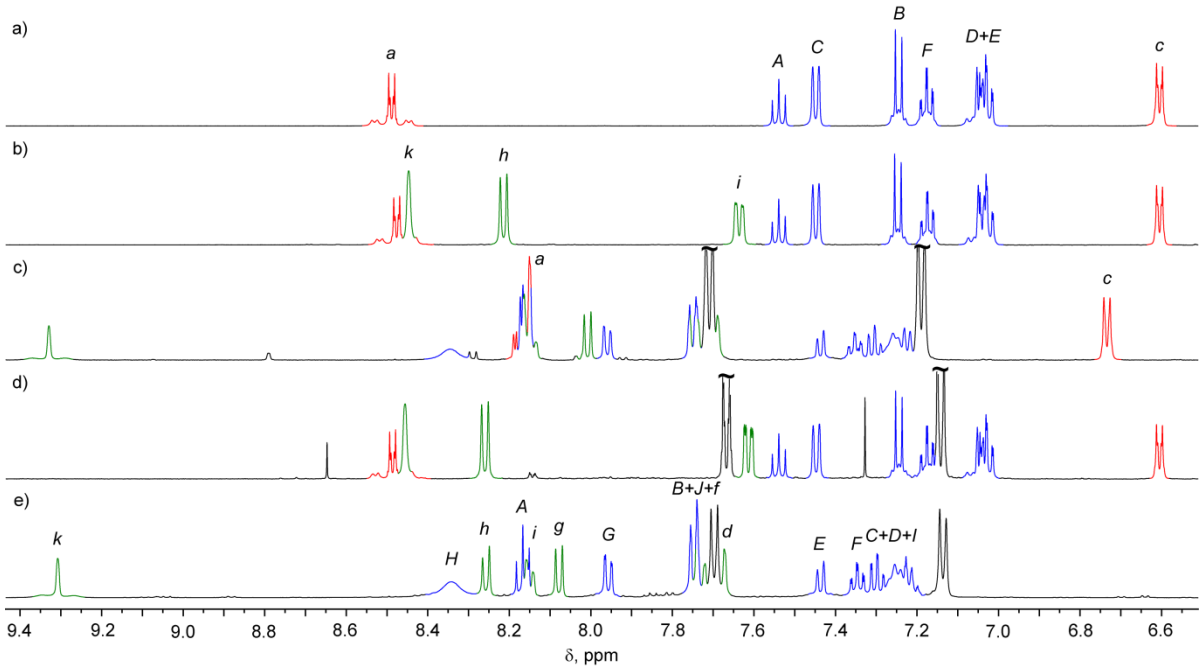

Figure S3. Partial ^{1}H NMR spectra (500 MHz, CD_2Cl_2, 298 K) of a) [**L**^{1}Pt(DMAP)]; b) [**L**^{1}Pt(DMAP)] + 5,5'-dimethyl-2,2'-bipyridine; c) [**L**^{1}Pt(DMAP)] + 5,5'-dimethyl-2,2'-bipyridine, 5 minutes after the addition of 2.7 eq. TsOH; d) 2 h after the subsequent addition of 5 eq. P_1-^{t}Bu; e) Authentic [H**L**^{1}Pt(dmbipy)]OTs (containing 3% CD_3OD). The assignments correspond to the lettering shown in Scheme S1 (page S10).

Acyclic ligand exchange experiments: Variation in acid quantity required to induce complete "3+1" to "2+2" switching.

In all the acyclic ligand exchange experiments, the minimum quantity of TsOH required to switch "3+1" to "2+2" complex was determined using titration-type experiments. When the monodentate ligand is pyridine, only a slight excess (1.3 eq.) was required, however, for 3,5-lut and DMAP, more equivalents were needed to induce complete switching. For example, Figure S4 shows a selection of the NMR spectra for the [**L**^{1}Pt(DMAP)]-dmbipy exchange experiment as a function of TsOH equivalents added.

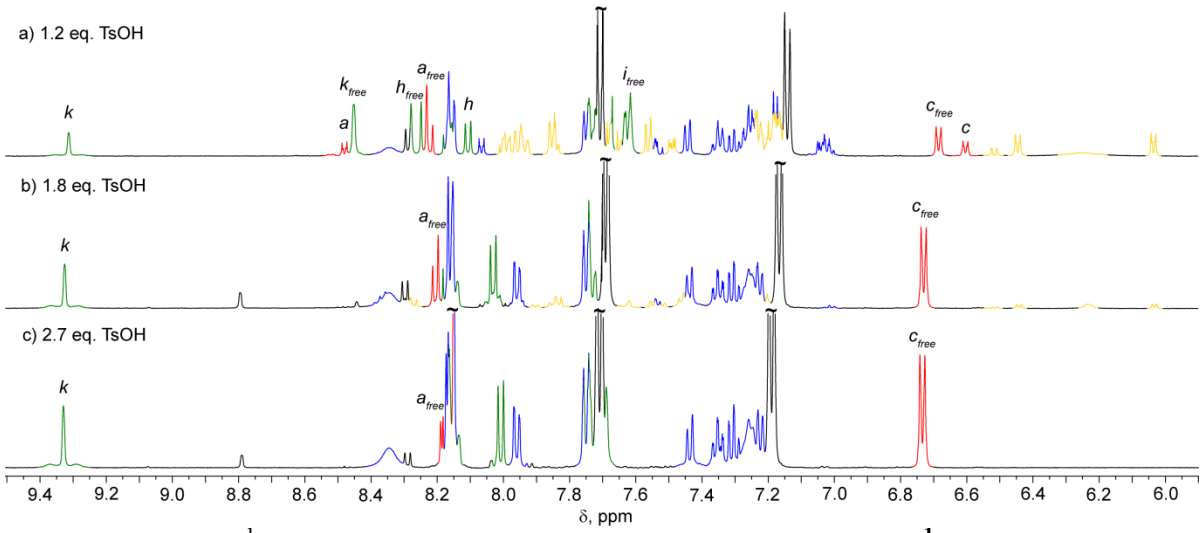

Figure S4. Partial ^{1}H NMR spectra (500 MHz, CD_2Cl_2, 298 K) of a) [**L**^{1}Pt(DMAP)] and dmbipy with a) 1.2; b) 1.8 and c) 2.7 eq. TsOH.

With a slight excess of TsOH (Figure S4a) both the "3+1" and "2+2" complexes are present, as well as "free" dmbipy and DMAP (protonated to various degrees), however, additional intermediate species can also be observed. For instance, the signal at 6.05 ppm is indicative of the protonated DMAP complex (the "2+1+1" species) [H**L**^{1}Pt(DMAP)OTs].[3] As the equivalents of TsOH (figures S4b and c) are increased we observe a reduction in both the "3+1" complex, **[L**^{1}Pt(DMAP)], and the intermediate [H**L**^{1}Pt(DMAP)OTs] and an increase in [H**L**^{1}Pt(dmbipy)]OTs. We attribute the difference in the amount of acid required to two principle effects. Firstly, liberated DMAP is significantly more basic than py (pKa of DMAP-H^{+} = 9.2, py-H^{+} = 5.21) such that free DMAP can cause the re-cyclometallation of the "2+2" complex. A further unpublished observation that supports this is that "3+1" complexes can be protonated by py-H^{+} but not by DMAP-H^{+}. The second effect is that DMAP is also a better ligand in comparison to py. In particular, the observation of [H**L**^{1}Pt(DMAP)OTs] suggests that the chelate effect of dmbipy is not sufficient to fully displace the strongly coordinating monodenate DMAP. The use of excess acid almost certainly shifts the equilibrium towards the "2+2" complex, [H**L**^{1}Pt(dmbipy)]OTs, through protonation of the liberated DMAP. Similar, but less pronounced, effects were observed for the exchange of **[L**^{1}Pt(3,5-lut)].

(ii)Macrocyclic Cyclometallated Pt Complexes

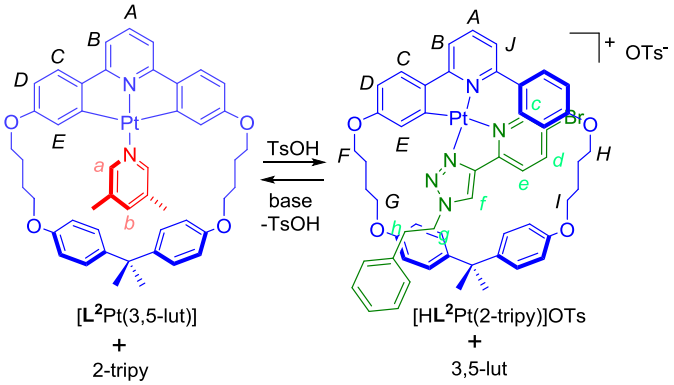

Scheme S2. Acid-Base responsive switching between "3+1" and "2+2" macrocyclic cyclometallated Pt complexes.

Procedure

To a solution of [$\mathbf{L}^2$Pt(3,5-lut)] (1.7 mg, 1.9 μmol) in CD_2Cl_2 (0.30 mL) at 298 K was added $\mathbf{L}^3$ (0.62 mg, 1.9 μmol). The subsequent addition TsOH in 97:3 CD_2Cl_2:CD_3OD (3.2 μmol) followed by agitation for 1 minute, caused the solution to lighten. A ^{1}H NMR spectrum was then recorded immediately, confirming complete conversion to [H$\mathbf{L}^2$Pt($\mathbf{L}^3$)]OTs. P_1-^{t}Bu in CD_2Cl_2 (9.5 μmol) was added directly to the NMR tube and the solution agitated for one minute. ^{1}H NMR spectra were recorded at regular intervals until no further change was observed, indicating that at 298 K, the backward reaction of macrocyclic "2+2" to "3+1" complex is complete after 48 h.

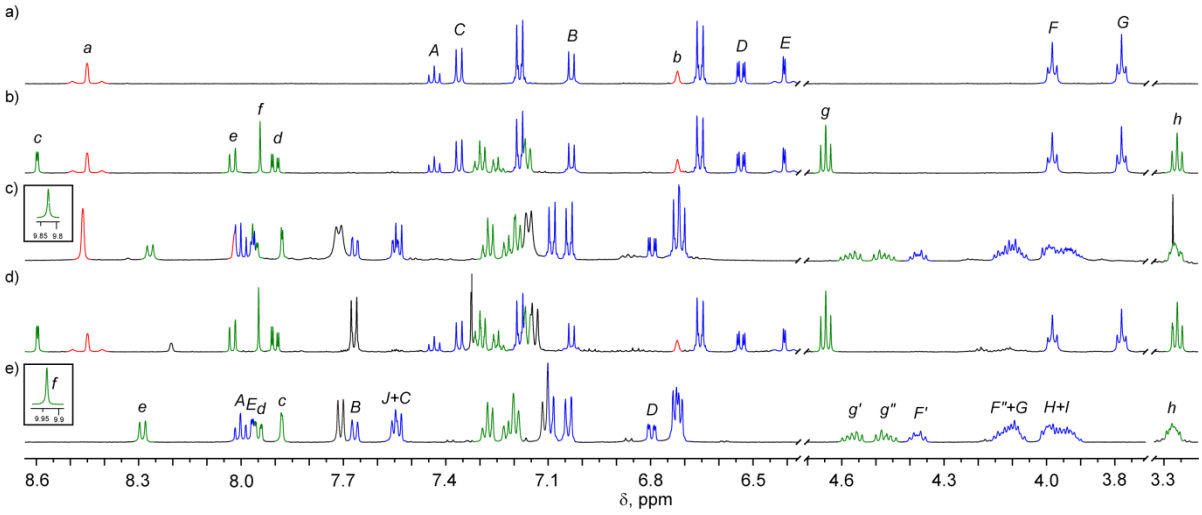

Figure S5. Partial ^{1}H NMR spectra (500 MHz, CD_2Cl_2, 298 K) of a) [$\mathbf{L}^2$Pt(3,5-lut)]; b) [$\mathbf{L}^2$Pt(3,5-lut)] + $\mathbf{L}^3$; c) [$\mathbf{L}^2$Pt(3,5-lut)] + $\mathbf{L}^3$, 5 minutes after the addition of 1.7 eq. TsOH; d) 48 h after the subsequent addition of 5 eq. P_1-^{t}Bu; e) Authentic [H$\mathbf{L}^2$Pt($\mathbf{L}^3$)]OTs. The assignments correspond to the lettering shown on pages S7 and S9. The assignments correspond to the lettering shown in Scheme S2 (page 14).

Crystal data and structure refinement for [L1Pt(3,5-Lut)], HL1Pt(dmbipy)]OTs, and [L2Pt(3,5-Lut)].

Structural data was collected using *Rigaku AFC12* goniometer equipped with an enhanced sensitivity (HG) *Saturn724+* detector mounted at the window of an *FR-E+ SuperBright* molybdenum rotating anode generator with VHF *Varimax* optics (70µm focus). Cell determination and data collection employed *CrystalClear-SM Expert 2.0 r11* (Rigaku, 2011). The structures were solved using *SHELXL97* (Sheldrick, G.M. (2008). Acta Cryst. A64, 112-122).

CCDC 956076-956078 contains the supplementary crystallographic data for this paper. This data can be obtained free of charge from The Cambridge Crystallographic Data Centre via www.ccdc.cam.ac.uk/data_request/cif.

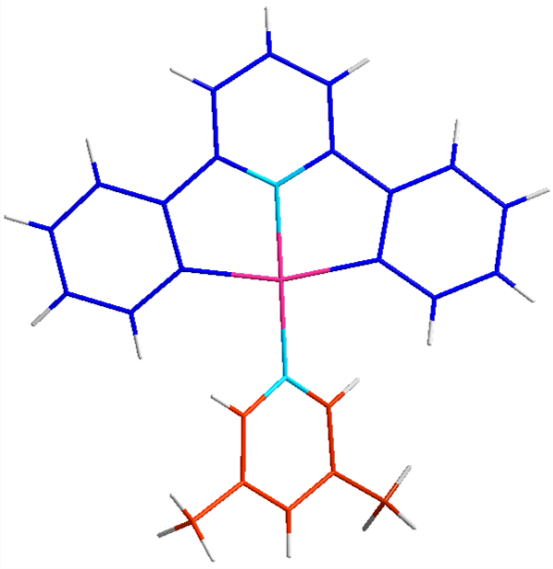

Figure S6. X-ray crystal structure of [**L**[1]Pt(3,5-Lut)]. The carbon atoms of CNC are shown in blue, Lut carbon in orange, platinum in pink, nitrogen in pale blue.

Table S1. Crystal data and structure refinement for [$\mathbf{L^1}$Pt(3,5-Lut)].

Identification code	[L1Pt(3,5-lut)]	
Empirical formula	C24 H20 N2 Pt	
Formula weight	531.51	
Temperature	93(2) K	
Wavelength	0.71073 Å	
Crystal system	Monoclinic	
Space group	P2(1)/n	
Unit cell dimensions	a = 7.402(2) Å	α= 90°.
	b = 18.424(5) Å	β= 90.431(10)°.
	c = 13.588(4) Å	γ = 90°.
Volume	1853.1(10) $Å^3$	
Z	4	
Density (calculated)	1.905 Mg/m^3	
Absorption coefficient	7.583 mm^{-1}	
F(000)	1024	
Crystal size	0.10 x 0.10 x 0.03 mm^3	
Theta range for data collection	1.86 to 25.33°	
Index ranges	-7<=h<=8, -18<=k<=22, -16<=l<=16	
Reflections collected	11348	
Independent reflections	3343 [R(int) = 0.0525]	
Completeness to theta = 25.00°	99.1 %	
Absorption correction	Multiscan	
Max. and min. transmission	1.000 and 0.579	
Refinement method	Full-matrix least-squares on F^2	
Data / restraints / parameters	3343 / 0 / 246	
Goodness-of-fit on F^2	1.064	
Final R indices [I>2sigma(I)]	R1 = 0.0302, wR2 = 0.0684	
R indices (all data)	R1 = 0.0414, wR2 = 0.0756	
Largest diff. peak and hole	1.467 and -2.092 $e.Å^{-3}$	

Table S2. Selected Bond lengths [Å] and angles [°] for [$\mathbf{L}^{1}$Pt(3,5-lut)].

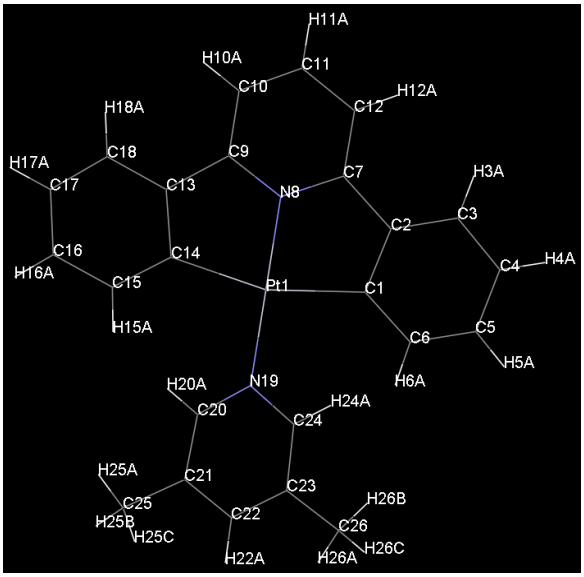

Pt(1)-N(8)	1.977(4)
Pt(1)-N(19)	2.030(4)
Pt(1)-C(1)	2.070(4)
Pt(1)-C(14)	2.073(4)
C(1)-C(6)	1.397(6)
C(1)-C(2)	1.425(6)
C(2)-C(3)	1.401(6)
C(2)-C(7)	1.468(6)
C(3)-C(4)	1.384(6)
C(3)-H(3A)	0.9500
C(4)-C(5)	1.380(6)
C(4)-H(4A)	0.9500
C(5)-C(6)	1.389(6)
C(5)-H(5A)	0.9500
C(6)-H(6A)	0.9500
C(7)-N(8)	1.372(5)
C(7)-C(12)	1.389(6)
N(8)-C(9)	1.361(6)
C(9)-C(10)	1.387(6)
C(9)-C(13)	1.481(6)
C(10)-C(11)	1.387(7)
C(10)-H(10A)	0.9500
C(11)-C(12)	1.388(7)
C(11)-H(11A)	0.9500
C(12)-H(12A)	0.9500

C(13)-C(18)	1.383(6)
C(13)-C(14)	1.427(6)
C(14)-C(15)	1.398(6)
C(15)-C(16)	1.384(6)
C(15)-H(15A)	0.9500
C(16)-C(17)	1.382(6)
C(16)-H(16A)	0.9500
C(17)-C(18)	1.389(6)
C(17)-H(17A)	0.9500
C(18)-H(18A)	0.9500
N(19)-C(20)	1.354(5)
N(19)-C(24)	1.359(6)
C(20)-C(21)	1.381(6)
C(20)-H(20A)	0.9500
C(21)-C(22)	1.401(6)
C(21)-C(25)	1.507(6)
C(22)-C(23)	1.380(7)
C(22)-H(22A)	0.9500
C(23)-C(24)	1.387(6)
C(23)-C(26)	1.496(6)
C(24)-H(24A)	0.9500
C(25)-H(25A)	0.9800
C(25)-H(25B)	0.9800
C(25)-H(25C)	0.9800
C(26)-H(26A)	0.9800
C(26)-H(26B)	0.9800
C(26)-H(26C)	0.9800

N(8)-Pt(1)-N(19)	178.70(15)
N(8)-Pt(1)-C(1)	81.25(16)
N(19)-Pt(1)-C(1)	98.60(16)
N(8)-Pt(1)-C(14)	80.80(15)
N(19)-Pt(1)-C(14)	99.33(15)
C(1)-Pt(1)-C(14)	162.02(17)
C(6)-C(1)-C(2)	115.7(4)
C(6)-C(1)-Pt(1)	133.2(3)
C(2)-C(1)-Pt(1)	111.1(3)
C(3)-C(2)-C(1)	121.7(4)
C(3)-C(2)-C(7)	121.9(4)

C(1)-C(2)-C(7)	116.4(4)
C(4)-C(3)-C(2)	119.8(4)
C(4)-C(3)-H(3A)	120.1
C(2)-C(3)-H(3A)	120.1
C(3)-C(4)-C(5)	119.9(4)
C(3)-C(4)-H(4A)	120.1
C(5)-C(4)-H(4A)	120.1
C(4)-C(5)-C(6)	120.1(4)
C(4)-C(5)-H(5A)	119.9
C(6)-C(5)-H(5A)	119.9
C(5)-C(6)-C(1)	122.7(4)
C(5)-C(6)-H(6A)	118.6
C(1)-C(6)-H(6A)	118.6
N(8)-C(7)-C(12)	118.6(4)
N(8)-C(7)-C(2)	112.9(4)
C(12)-C(7)-C(2)	128.5(4)
C(9)-N(8)-C(7)	122.6(4)
C(9)-N(8)-Pt(1)	119.1(3)
C(7)-N(8)-Pt(1)	118.2(3)
N(8)-C(9)-C(10)	118.9(4)
N(8)-C(9)-C(13)	112.6(4)
C(10)-C(9)-C(13)	128.5(4)
C(11)-C(10)-C(9)	120.0(5)
C(11)-C(10)-H(10A)	120.0
C(9)-C(10)-H(10A)	120.0
C(10)-C(11)-C(12)	119.9(5)
C(10)-C(11)-H(11A)	120.1
C(12)-C(11)-H(11A)	120.1
C(11)-C(12)-C(7)	119.9(4)
C(11)-C(12)-H(12A)	120.1
C(7)-C(12)-H(12A)	120.1
C(18)-C(13)-C(14)	122.8(4)
C(18)-C(13)-C(9)	121.4(4)
C(14)-C(13)-C(9)	115.8(4)
C(15)-C(14)-C(13)	114.8(4)
C(15)-C(14)-Pt(1)	133.7(3)
C(13)-C(14)-Pt(1)	111.5(3)
C(16)-C(15)-C(14)	123.0(4)
C(16)-C(15)-H(15A)	118.5

C(14)-C(15)-H(15A)	118.5
C(17)-C(16)-C(15)	120.0(4)
C(17)-C(16)-H(16A)	120.0
C(15)-C(16)-H(16A)	120.0
C(16)-C(17)-C(18)	119.9(4)
C(16)-C(17)-H(17A)	120.1
C(18)-C(17)-H(17A)	120.1
C(13)-C(18)-C(17)	119.4(4)
C(13)-C(18)-H(18A)	120.3
C(17)-C(18)-H(18A)	120.3
C(20)-N(19)-C(24)	116.5(4)
C(20)-N(19)-Pt(1)	121.3(3)
C(24)-N(19)-Pt(1)	122.1(3)
N(19)-C(20)-C(21)	124.3(4)
N(19)-C(20)-H(20A)	117.8
C(21)-C(20)-H(20A)	117.8
C(20)-C(21)-C(22)	117.1(4)
C(20)-C(21)-C(25)	121.3(4)
C(22)-C(21)-C(25)	121.7(4)
C(23)-C(22)-C(21)	120.6(4)
C(23)-C(22)-H(22A)	119.7
C(21)-C(22)-H(22A)	119.7
C(22)-C(23)-C(24)	117.8(4)
C(22)-C(23)-C(26)	121.7(4)
C(24)-C(23)-C(26)	120.5(4)
N(19)-C(24)-C(23)	123.6(4)
N(19)-C(24)-H(24A)	118.2
C(23)-C(24)-H(24A)	118.2
C(21)-C(25)-H(25A)	109.5
C(21)-C(25)-H(25B)	109.5
H(25A)-C(25)-H(25B)	109.5
C(21)-C(25)-H(25C)	109.5
H(25A)-C(25)-H(25C)	109.5
H(25B)-C(25)-H(25C)	109.5
C(23)-C(26)-H(26A)	109.5
C(23)-C(26)-H(26B)	109.5
H(26A)-C(26)-H(26B)	109.5
C(23)-C(26)-H(26C)	109.5
H(26A)-C(26)-H(26C)	109.5

H(26B)-C(26)-H(26C) 109.5

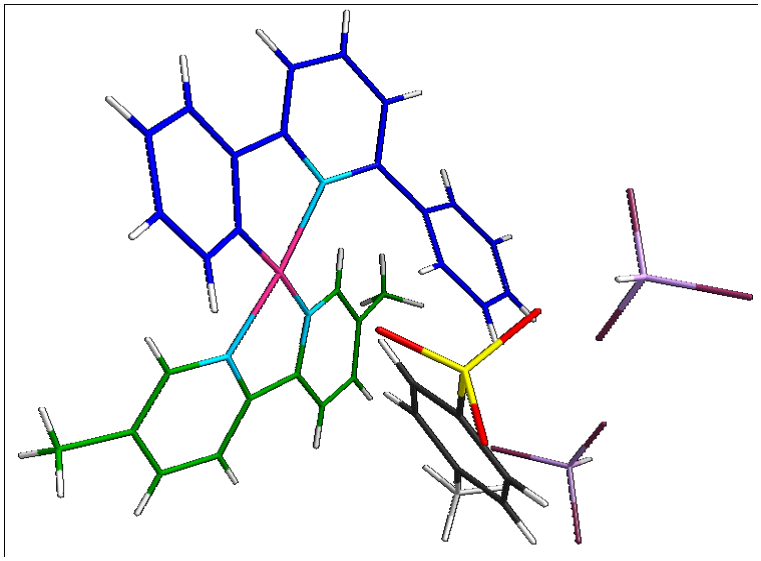

Figure S7. X-ray crystal structure of [H**L**[1]Pt(dmbipy)]OTs.2CHCl$_3$. The carbon atoms of CNC are shown in blue, dmbpy in dark green and OTs carbon in dark grey, platinum in pink, nitrogen in pale blue, sulfur in yellow, oxygen in red and chlorine in purple.

Table S3. Crystal data and structure refinement for [H**L**[1]Pt(dmbipy)]OTs.2CHCl$_3$.

Identification code	[HL1Pt(dibipy)]	
Empirical formula	C38 H33 Cl6 N3 O3 Pt S	
Formula weight	1019.52	
Temperature	93(2) K	
Wavelength	0.71073 Å	
Crystal system	Monoclinic	
Space group	P2(1)/c	
Unit cell dimensions	a = 16.521(4) Å	α= 90°.
	b = 14.330(3) Å	β= 115.215(5)°.
	c = 17.844(4) Å	γ = 90°.
Volume	3821.8(14) Å^3	
Z	4	
Density (calculated)	1.772 mg/m^3	
Absorption coefficient	4.188 mm^{-1}	
F(000)	2008	
Crystal size	0.10 x 0.06 x 0.06 mm^3	
Theta range for data collection	2.30 to 25.36°	
Index ranges	-18<=h<=19, -13<=k<=17, -20<=l<=21	
Reflections collected	23501	
Independent reflections	6874 [R(int) = 0.0535]	

Completeness to theta = 25.00°	98.6 %
Absorption correction	Multiscan
Max. and min. transmission	1.0000 and 0.725
Refinement method	Full-matrix least-squares on F^2
Data / restraints / parameters	6874 / 6 / 472
Goodness-of-fit on F^2	1.116
Final R indices [I>2sigma(I)]	R1 = 0.0606, wR2 = 0.1515
R indices (all data)	R1 = 0.0696, wR2 = 0.1583
Largest diff. peak and hole	2.479 and -2.569 e.Å^{-3}

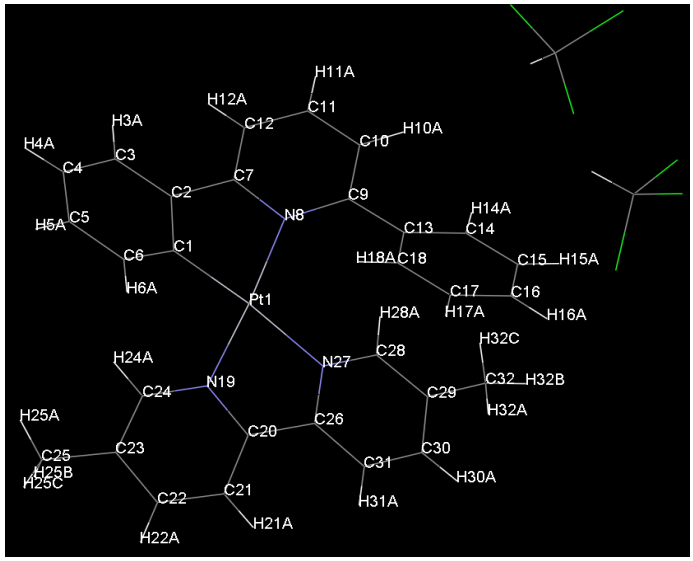

Table S4. Selected Bond lengths [Å] and angles [°] for [H**L**^{1}Pt(dmbipy)]OTs.2CHCl$_3$.

Pt(1)-C(1)	1.997(9)
Pt(1)-N(19)	2.027(7)
Pt(1)-N(8)	2.063(7)
Pt(1)-N(27)	2.137(7)
C(1)-C(6)	1.383(13)
C(1)-C(2)	1.426(12)
C(2)-C(3)	1.398(12)
C(2)-C(7)	1.463(12)
C(3)-C(4)	1.397(13)
C(3)-H(3A)	0.9500
C(4)-C(5)	1.403(13)
C(4)-H(4A)	0.9500
C(5)-C(6)	1.384(13)
C(5)-H(5A)	0.9500
C(6)-H(6A)	0.9500
C(7)-C(12)	1.378(12)

C(7)-N(8)	1.375(11)
N(8)-C(9)	1.384(12)
C(9)-C(10)	1.397(13)
C(9)-C(13)	1.467(14)
C(10)-C(11)	1.372(13)
C(10)-H(10A)	0.9500
C(11)-C(12)	1.379(13)
C(11)-H(11A)	0.9500
C(12)-H(12A)	0.9500
C(13)-C(18)	1.393(13)
C(13)-C(14)	1.420(13)
C(14)-C(15)	1.365(15)
C(14)-H(14A)	0.9500
C(15)-C(16)	1.359(16)
C(15)-H(15A)	0.9500
C(16)-C(17)	1.414(15)
C(16)-H(16A)	0.9500
C(17)-C(18)	1.389(14)
C(17)-H(17A)	0.9500
C(18)-H(18A)	0.9500
N(19)-C(24)	1.350(11)
N(19)-C(20)	1.361(11)
C(20)-C(21)	1.394(12)
C(20)-C(26)	1.467(12)
C(21)-C(22)	1.382(13)
C(21)-H(21A)	0.9500
C(22)-C(23)	1.386(13)
C(22)-H(22A)	0.9500
C(23)-C(24)	1.367(12)
C(23)-C(25)	1.526(13)
C(24)-H(24A)	0.9500
C(25)-H(25A)	0.9800
C(25)-H(25B)	0.9800
C(25)-H(25C)	0.9800
C(26)-N(27)	1.369(11)
C(26)-C(31)	1.383(12)
N(27)-C(28)	1.332(11)
C(28)-C(29)	1.392(12)
C(28)-H(28A)	0.9500

C(29)-C(30)	1.391(13)
C(29)-C(32)	1.504(13)
C(30)-C(31)	1.391(13)
C(30)-H(30A)	0.9500
C(31)-H(31A)	0.9500
C(32)-H(32A)	0.9800
C(32)-H(32B)	0.9800
C(32)-H(32C)	0.9800

C(1)-Pt(1)-N(19)	98.2(3)
C(1)-Pt(1)-N(8)	79.6(3)
N(19)-Pt(1)-N(8)	174.3(3)
C(1)-Pt(1)-N(27)	174.6(3)
N(19)-Pt(1)-N(27)	77.6(3)
N(8)-Pt(1)-N(27)	104.3(3)
C(6)-C(1)-C(2)	117.2(8)
C(6)-C(1)-Pt(1)	131.8(7)
C(2)-C(1)-Pt(1)	110.9(6)
C(3)-C(2)-C(1)	121.0(8)
C(3)-C(2)-C(7)	124.1(8)
C(1)-C(2)-C(7)	114.4(8)
C(2)-C(3)-C(4)	119.7(8)
C(2)-C(3)-H(3A)	120.2
C(4)-C(3)-H(3A)	120.2
C(5)-C(4)-C(3)	119.1(8)
C(5)-C(4)-H(4A)	120.5
C(3)-C(4)-H(4A)	120.5
C(6)-C(5)-C(4)	120.5(9)
C(6)-C(5)-H(5A)	119.8
C(4)-C(5)-H(5A)	119.8
C(1)-C(6)-C(5)	121.8(9)
C(1)-C(6)-H(6A)	119.1
C(5)-C(6)-H(6A)	119.1
C(12)-C(7)-N(8)	121.5(8)
C(12)-C(7)-C(2)	124.9(8)
N(8)-C(7)-C(2)	113.4(7)
C(7)-N(8)-C(9)	118.1(8)
C(7)-N(8)-Pt(1)	110.9(6)
C(9)-N(8)-Pt(1)	130.6(6)

N(8)-C(9)-C(10)	119.4(9)
N(8)-C(9)-C(13)	119.7(8)
C(10)-C(9)-C(13)	120.8(8)
C(11)-C(10)-C(9)	120.9(9)
C(11)-C(10)-H(10A)	119.6
C(9)-C(10)-H(10A)	119.6
C(10)-C(11)-C(12)	119.1(8)
C(10)-C(11)-H(11A)	120.5
C(12)-C(11)-H(11A)	120.5
C(7)-C(12)-C(11)	119.7(8)
C(7)-C(12)-H(12A)	120.2
C(11)-C(12)-H(12A)	120.2
C(18)-C(13)-C(14)	118.3(9)
C(18)-C(13)-C(9)	122.2(9)
C(14)-C(13)-C(9)	119.6(9)
C(15)-C(14)-C(13)	119.8(10)
C(15)-C(14)-H(14A)	120.1
C(13)-C(14)-H(14A)	120.1
C(14)-C(15)-C(16)	121.9(10)
C(14)-C(15)-H(15A)	119.0
C(16)-C(15)-H(15A)	119.0
C(15)-C(16)-C(17)	120.0(10)
C(15)-C(16)-H(16A)	120.0
C(17)-C(16)-H(16A)	120.0
C(18)-C(17)-C(16)	118.6(10)
C(18)-C(17)-H(17A)	120.7
C(16)-C(17)-H(17A)	120.7
C(13)-C(18)-C(17)	121.3(9)
C(13)-C(18)-H(18A)	119.3
C(17)-C(18)-H(18A)	119.3
C(24)-N(19)-C(20)	117.7(8)
C(24)-N(19)-Pt(1)	125.7(6)
C(20)-N(19)-Pt(1)	116.6(6)
N(19)-C(20)-C(21)	120.9(8)
N(19)-C(20)-C(26)	115.1(8)
C(21)-C(20)-C(26)	123.2(8)
C(22)-C(21)-C(20)	119.9(8)
C(22)-C(21)-H(21A)	120.0
C(20)-C(21)-H(21A)	120.0

C(21)-C(22)-C(23)	119.0(8)
C(21)-C(22)-H(22A)	120.5
C(23)-C(22)-H(22A)	120.5
C(24)-C(23)-C(22)	118.4(9)
C(24)-C(23)-C(25)	120.7(9)
C(22)-C(23)-C(25)	120.9(8)
N(19)-C(24)-C(23)	124.1(8)
N(19)-C(24)-H(24A)	118.0
C(23)-C(24)-H(24A)	117.9
C(23)-C(25)-H(25A)	109.5
C(23)-C(25)-H(25B)	109.5
H(25A)-C(25)-H(25B)	109.5
C(23)-C(25)-H(25C)	109.5
H(25A)-C(25)-H(25C)	109.5
H(25B)-C(25)-H(25C)	109.5
N(27)-C(26)-C(31)	120.9(8)
N(27)-C(26)-C(20)	114.3(8)
C(31)-C(26)-C(20)	124.6(8)
C(28)-N(27)-C(26)	118.7(7)
C(28)-N(27)-Pt(1)	128.9(6)
C(26)-N(27)-Pt(1)	112.2(6)
N(27)-C(28)-C(29)	123.5(8)
N(27)-C(28)-H(28A)	118.2
C(29)-C(28)-H(28A)	118.2
C(28)-C(29)-C(30)	117.2(8)
C(28)-C(29)-C(32)	121.5(8)
C(30)-C(29)-C(32)	121.2(8)
C(31)-C(30)-C(29)	119.8(8)
C(31)-C(30)-H(30A)	120.1
C(29)-C(30)-H(30A)	120.1
C(26)-C(31)-C(30)	119.3(8)
C(26)-C(31)-H(31A)	120.3
C(30)-C(31)-H(31A)	120.3
C(29)-C(32)-H(32A)	109.5
C(29)-C(32)-H(32B)	109.5
H(32A)-C(32)-H(32B)	109.5
C(29)-C(32)-H(32C)	109.5
H(32A)-C(32)-H(32C)	109.5
H(32B)-C(32)-H(32C)	109.5

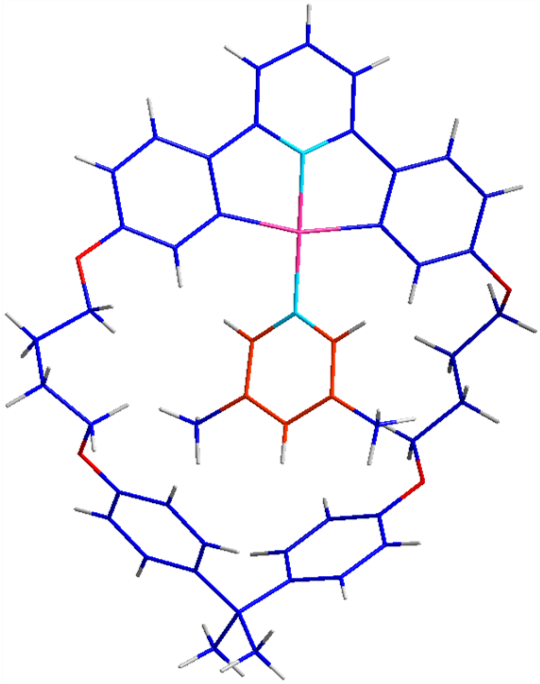

Figure S8. X-ray crystal structure of [$\mathbf{L}^2$Pt(3,5-Lut)]. The carbon atoms of a macrocycle are shown in blue, Lut in orange, platinum in pink, nitrogen in pale blue, and oxygen in red.

Table S5. Crystal data and structure refinement for [$\mathbf{L}^2$Pt(3,5-Lut)].

Identification code	[L2Pt(3,5-lut)]	
Empirical formula	C47 H48 N2 O4 Pt	
Formula weight	900.00	
Temperature	93(2) K	
Wavelength	0.71075 Å	
Crystal system	Triclinic	
Space group	P-1 (#2)	
Unit cell dimensions	a = 10.3265(10) Å	α = 110.841(6)°
	b = 13.6884(13) Å	β = 107.420(5)°
	c = 15.3966(12) Å	γ = 95.035(5)°
Volume	1894.1(3) $Å^3$	
Z	2	
Density (calculated)	1.578 g/cm^3	
Absorption coefficient	3.7379 mm^{-1}	
F(000)	908.00	
Crystal size	0.10 x 0.03 x 0.03 mm^3	
Theta range for data collection	2.38 to 25.35°	
Index ranges	-12<=h<=12, -16<=k<=16, -18<=l<=18	
Reflections collected	18722	
Independent reflections	6861 [R(int) = 0.0261]	
Completeness to theta = 25.00°	98.5%	

Absorption correction	Multiscan
Max. and min. transmission	0.894 and 0.760
Refinement method	Full-matrix least-squares on F^2
Data / restraints / parameters	6861/ 0 / 487
Goodness-of-fit on F^2	1.199
Final R indices [I>2sigma(I)]	R1 = 0.0234
R indices (all data)	wR2 = 0.0771
Largest diff. peak and hole	1.050 and -1.030 e. $Å^{-3}$

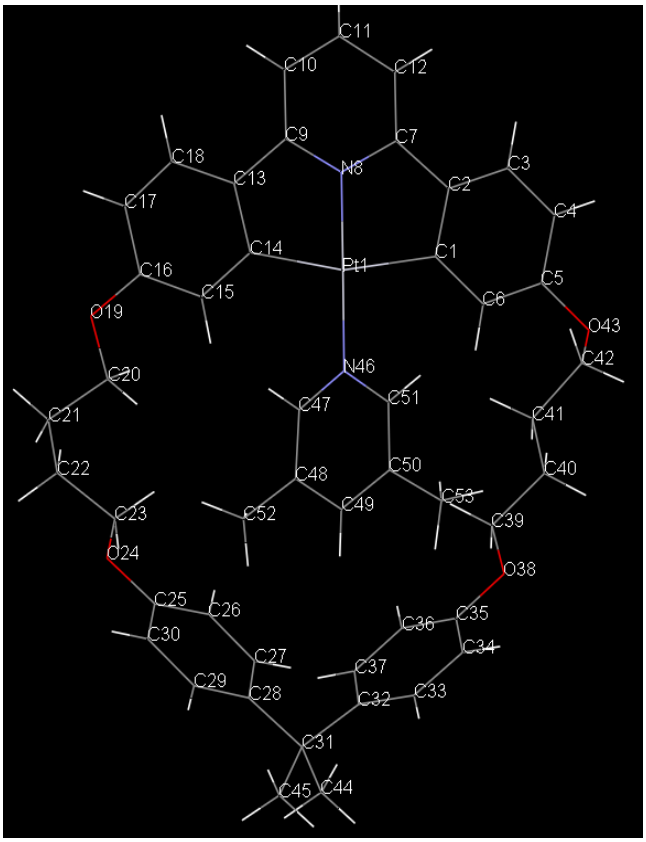

Table S6. Selected Bond lengths [Å], angles [°] and torsion angles [°] for [$\mathbf{L^2}$Pt(3,5-Lut)].

Pt(1)-N(8)	1.956(4)
Pt(1)-C(14)	2.046(6)
Pt(1)-C(1)	2.063(6)
Pt(1)-N(46)	2.010(4)
C(1)-C(2)	1.401(8)
C(1)-C(6)	1.405(7)
C(6)-C(5)	1.39(1)
C(5)-C(4)	1.393(8)
C(4)-C(3)	1.382(7)
C(3)-C(2)	1.39(1)
C(2)-C(7)	1.473(7)
C(7)-C(12)	1.381(8)
C(12)-C(11)	1.385(8)

C(11)-C(10)	1.40(1)
C(10)-C(9)	1.382(8)
N(8)-C(9)	1.359(7)
N(8)-C(7)	1.376(9)
C(9)-C(13)	1.468(9)
C(13)-C(14)	1.417(6)
C(13)-C(18)	1.401(8)
C(18)-C(17)	1.38(1)
C(17)-C(16)	1.392(7)
C(16)-C(15)	1.389(8)
C(15)-C(14)	1.410(9)
N(46)-C(47)	1.354(7)
N(46)-C(51)	1.348(7)
C(51)-C(50)	1.366(8)
C(50)-C(49)	1.404(8)
C(49)-C(48)	1.392(8)
C(48)-C(47)	1.379(8)
H(53B)-C(53)	0.980(5)
C(52)-C(48)	1.506(8)
C(16)-O(19)	1.378(8)
C(21)-C(22)	1.524(9)
C(22)-C(23)	1.520(7)
C(23)-O(24)	1.434(5)
O(24)-C(25)	1.383(6)
C(25)-C(26)	1.398(8)
C(26)-C(27)	1.390(7)
C(27)-C(28)	1.389(6)
C(28)-C(29)	1.398(8)
C(29)-C(30)	1.393(7)
C(30)-C(25)	1.373(6)
C(28)-C(31)	1.538(7)
C(31)-C(32)	1.55(1)
C(31)-C(44)	1.544(9)
C(31)-C(45)	1.536(6)
C(32)-C(33)	1.380(8)
C(32)-C(37)	1.389(9)
C(37)-C(36)	1.39(1)
C(36)-C(35)	1.386(8)
C(35)-C(34)	1.387(9)
C(34)-C(33)	1.40(1)
C(35)-O(38)	1.377(8)

O(38)-C(39)	1.438(8)
C(39)-C(40)	1.511(9)
C(40)-C(41)	1.525(9)
C(41)-C(42)	1.514(9)
O(43)-C(5)	1.391(6)
O(43)-C(42)	1.450(6)
C(28)-C(52)	4.105(8)
C(52)-C(25)	3.783(9)
C(53)-C(32)	4.755(7)
C(35)-C(53)	3.600(6)
C(48)-C(27)	4.507(9)
C(48)-C(26)	4.39(1)
C(48)-C(30)	4.546(9)
C(48)-C(29)	4.668(9)
C(53)-C(37)	4.893(6)
C(36)-C(53)	4.392(6)
C(33)-C(53)	4.054(7)
C(34)-C(53)	3.402(6)
C(20)-C(21)	1.499(9)
C(20)-O(19)	1.437(7)

N(46)-Pt(1)-C(14)	99.0(2)
N(46)-Pt(1)-C(1)	98.5(2)
Pt(1)-C(14)-C(13)	111.9(4)
C(14)-C(13)-C(9)	115.4(5)
C(9)-N(8)-C(7)	123.1(5)
C(9)-N(8)-Pt(1)	118.9(4)
C(7)-N(8)-Pt(1)	118.0(4)
C(7)-C(2)-C(1)	116.1(5)
C(6)-C(5)-O(43)	120.2(5)
C(5)-O(43)-C(42)	114.9(4)
O(43)-C(42)-C(41)	113.8(5)
C(42)-C(41)-C(40)	113.7(5)
C(40)-C(39)-O(38)	108.4(5)
C(39)-O(38)-C(35)	117.6(4)
C(52)-C(48)-C(47)	120.4(5)
C(47)-N(46)-C(51)	117.4(5)
C(51)-C(50)-H(39B)	93.3(3)
C(16)-O(19)-C(20)	117.5(4)
C(15)-C(16)-O(19)	123.7(5)
C(20)-C(21)-C(22)	112.7(5)

C(22)-C(23)-O(24)	108.8(5)
C(23)-O(24)C(25)	117.7(4)
O(24)-C(25)C(26)	123.7(5)
O(24)-C(25)C(30)	116.9(5)
C(29)-C(28)-C(31)	123.2(5)
C(37)-C(32)-C(31)	119.8(5)

C(14)-Pt(1)-N(46)-C(47)	-51.7(4)
C(12)-C(7)-C(2)-C(3)	-1(1)
C(10)-C(9)-C(13)-C(18)	-1.0(9)
C(6)-C(1)-Pt(1)-N(46)	-3.6(6)
C(15)-C(16)-O(19)-C(20)	-24.7(8)
C(16)-O(19)-C(20)-H(21B)	147.6(4)
C(20)-C(21)-C(22)-O(24)	82.3(5)
Pt(1)-N(46)-C(51)-C(1)	33.1(2)
C(33)-C(32)-C(31)-C(28)	-105.1(6)
C(31)-C(28)-C(27)-C(37)	-61.2(4)
C(26)-C(25)-O(24)-C(23)	-1.6(8)
C(34)-C(35)-O(38)-C(39)	164.6(5)
O(38)-C(39)-C(40)-C(41)	177.1(5)
C(6)-C(5)C(42)-C(41)	1.0(6)

^{1}H and ^{13}C NMR Spectra of all new compounds and complexes

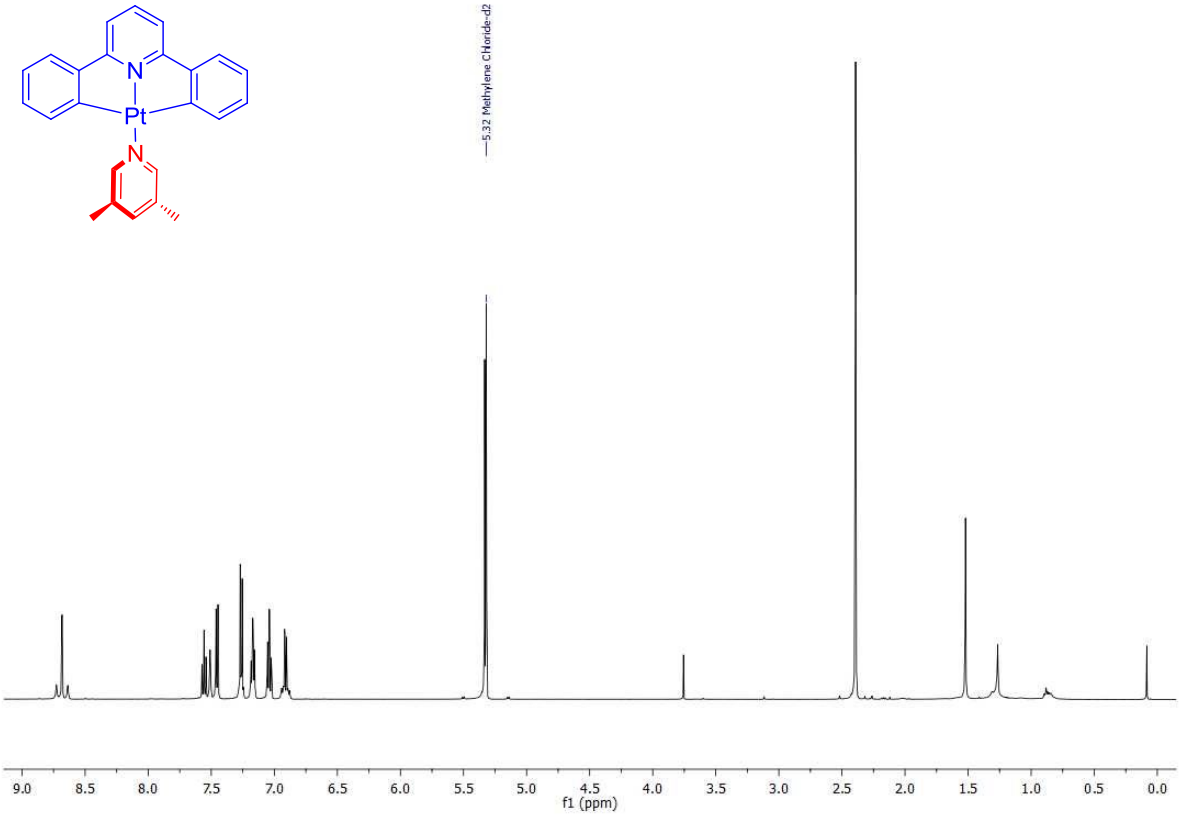

Figure S9. ^{1}H NMR spectrum (500 MHz, CD_2Cl_2, 298 K) of [**L**^{1}Pt(3,5-Lut)].

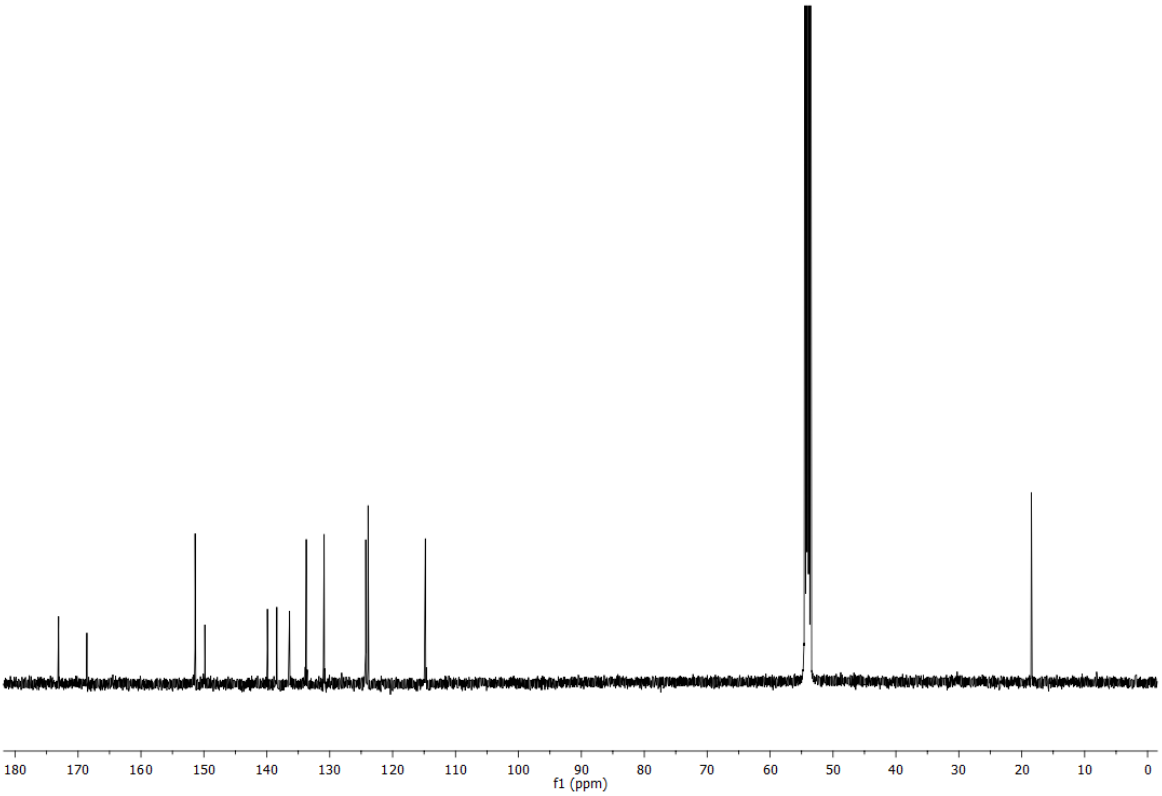

Figure S10. ^{13}C NMR spectrum (125 MHz, CD_2Cl_2, 298 K) of [**L**^{1}Pt(3,5-Lut)].

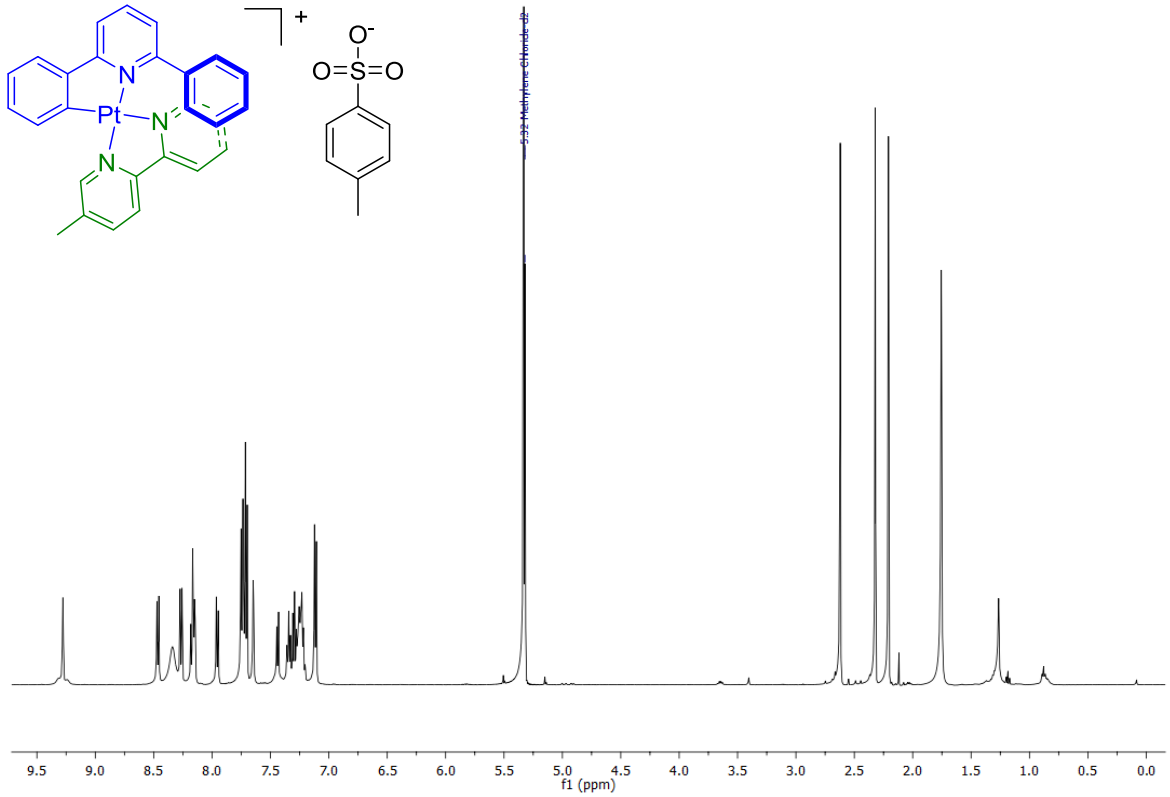

Figure S11. ^{1}H NMR spectrum (500 MHz, CD_2Cl_2, 298 K) of [H**L**^{1}Pt(dmbipy)]OTs.

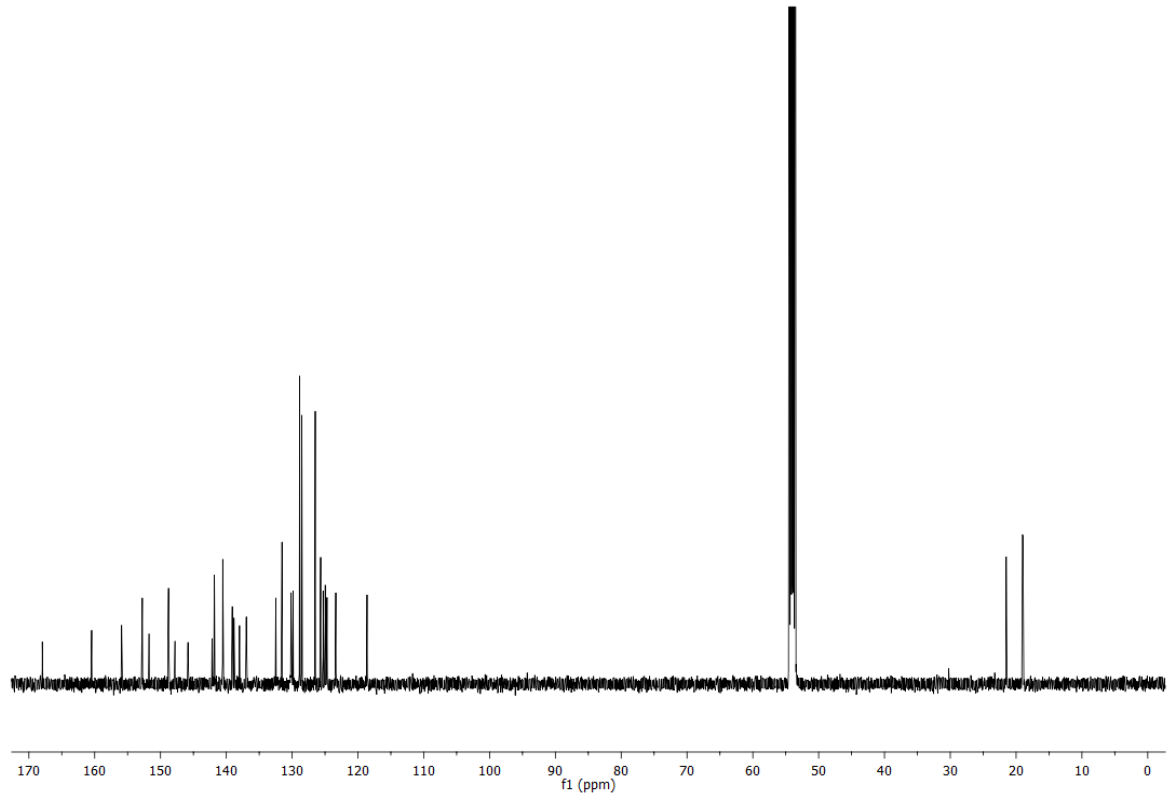

Figure S12. ^{13}C NMR spectrum (125 MHz, CD_2Cl_2, 298 K) of [H**L**^{1}Pt(dmbipy)]OTs.

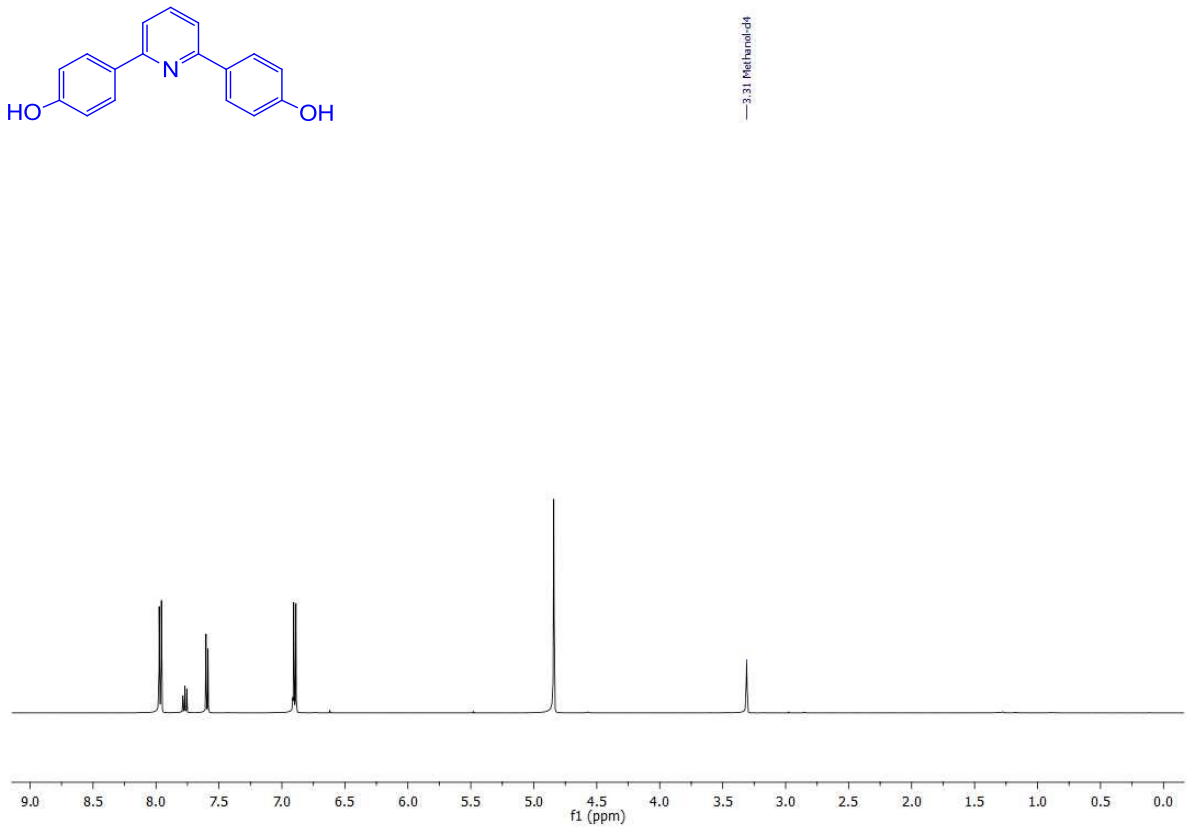

Figure S13. ^{1}H NMR spectrum (500 MHz, CD_3OD, 298 K) of 2,6-(bis-4-hydroxyphenyl)pyridine.

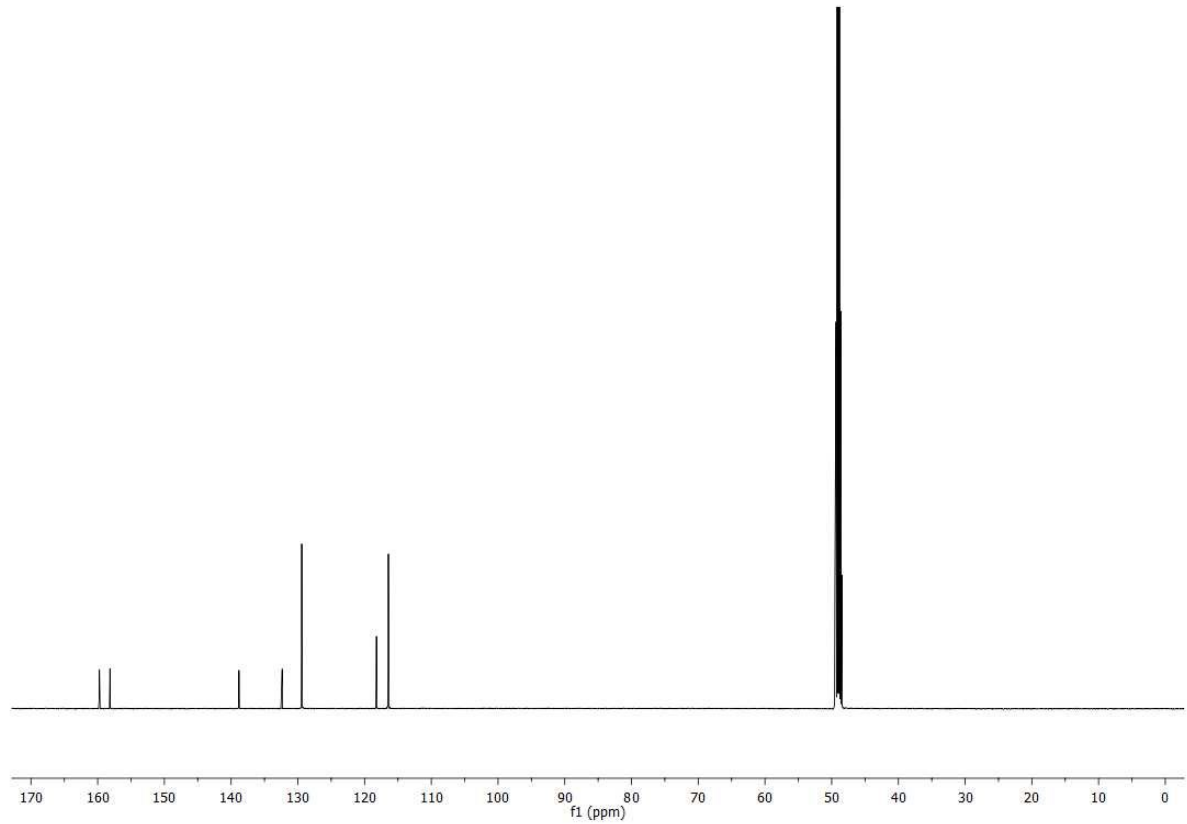

Figure S14. ^{13}C NMR spectrum (125 MHz, CD_3OD, 298 K) of 2,6-(bis-4-hydroxyphenyl)pyridine.

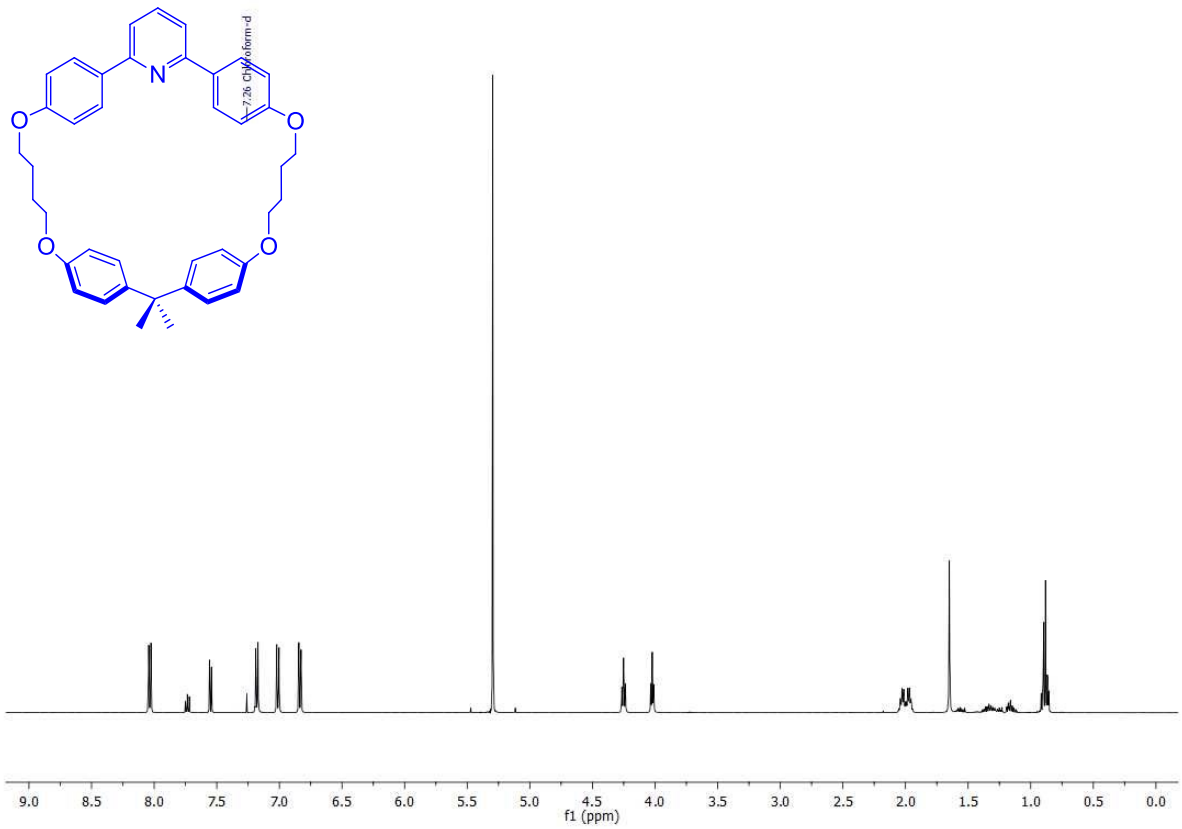

Figure S15. ^{1}H NMR spectrum (500 MHz, $CDCl_3$, 298 K) of $H_2\mathbf{L}^{\mathbf{2}}$.

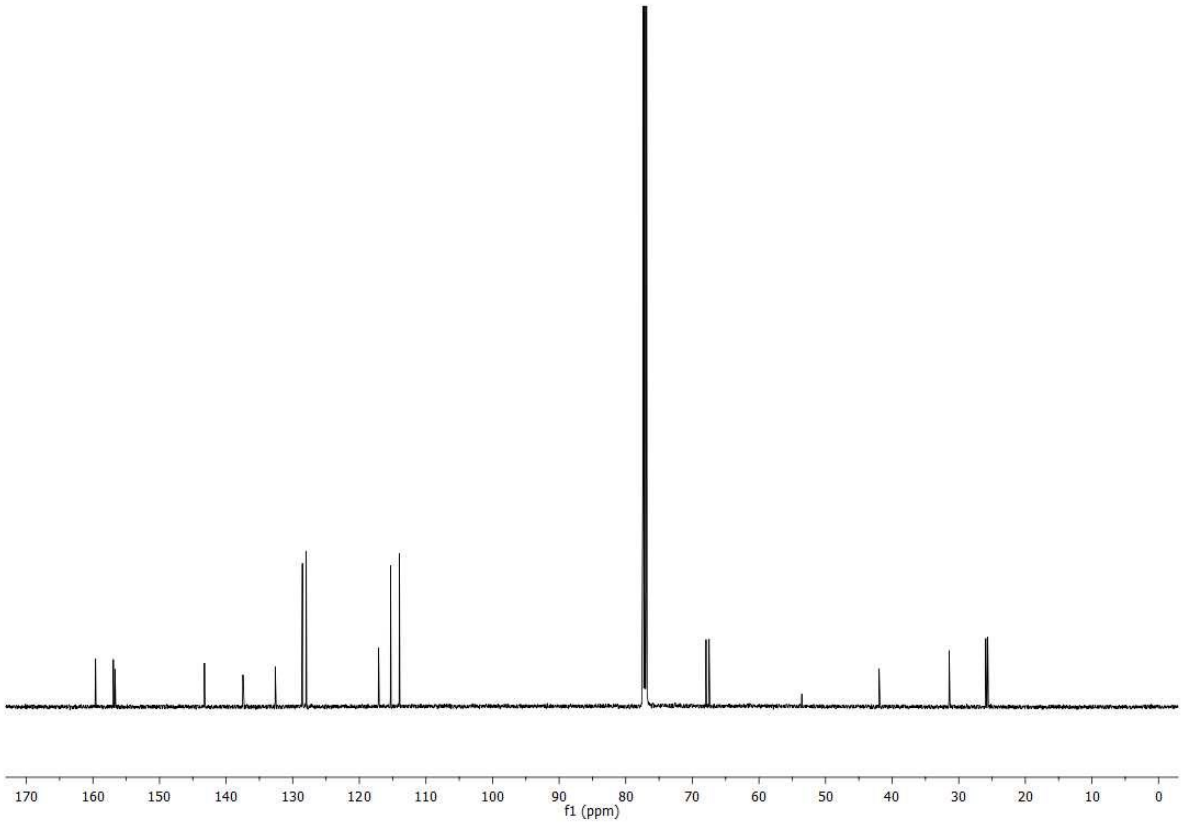

Figure S16. ^{13}C NMR spectrum (125 MHz, $CDCl_3$, 298 K) of $H_2\mathbf{L}^{\mathbf{2}}$.

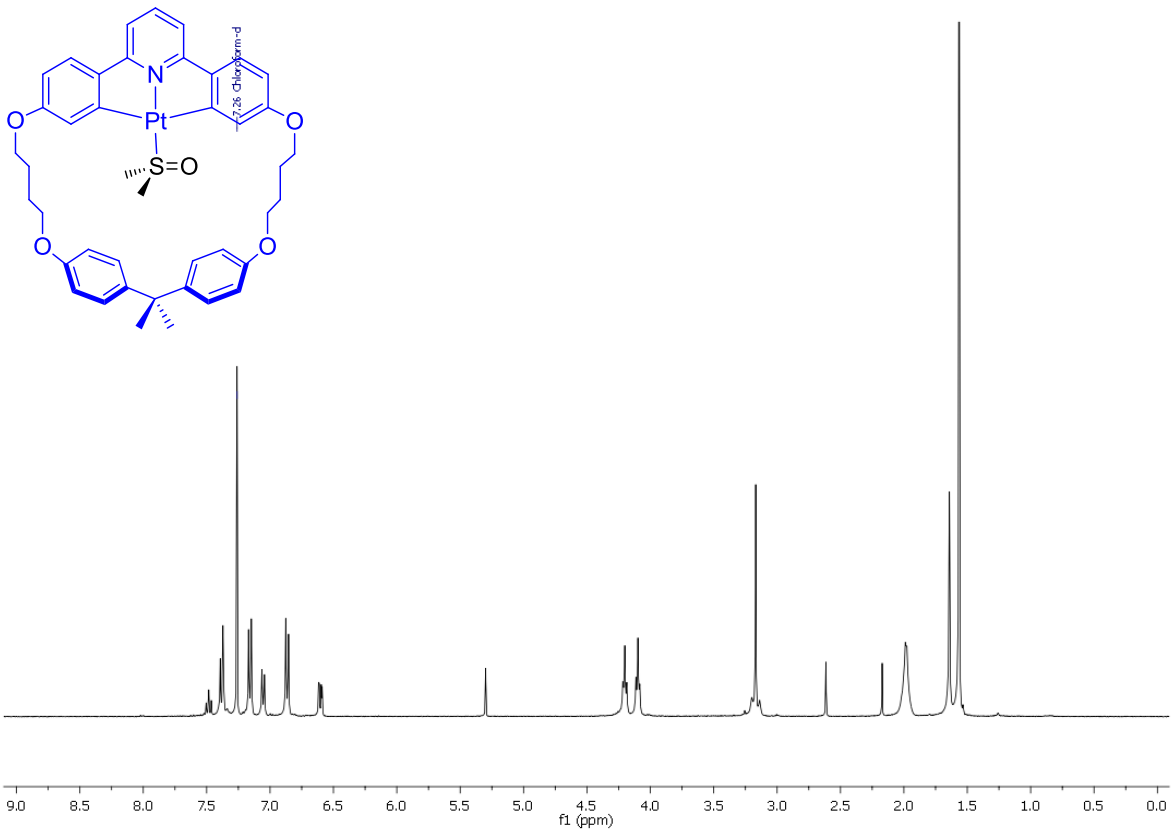

Figure S17. ^{1}H NMR spectrum (500 MHz, $CDCl_3$, 298 K) of [$\mathbf{L^2}$Pt(DMSO)].

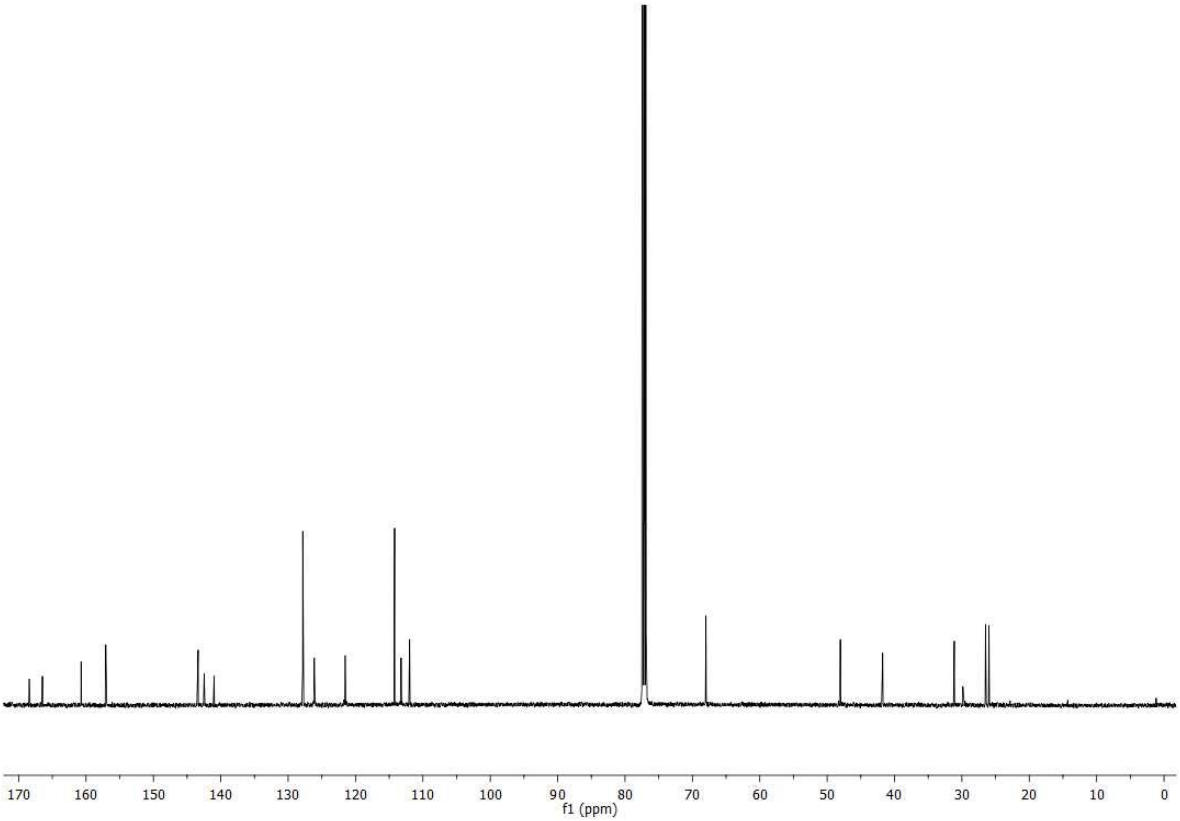

Figure S18. ^{13}C NMR spectrum (125 MHz, $CDCl_3$, 298 K) of [$\mathbf{L^2}$Pt(DMSO)].

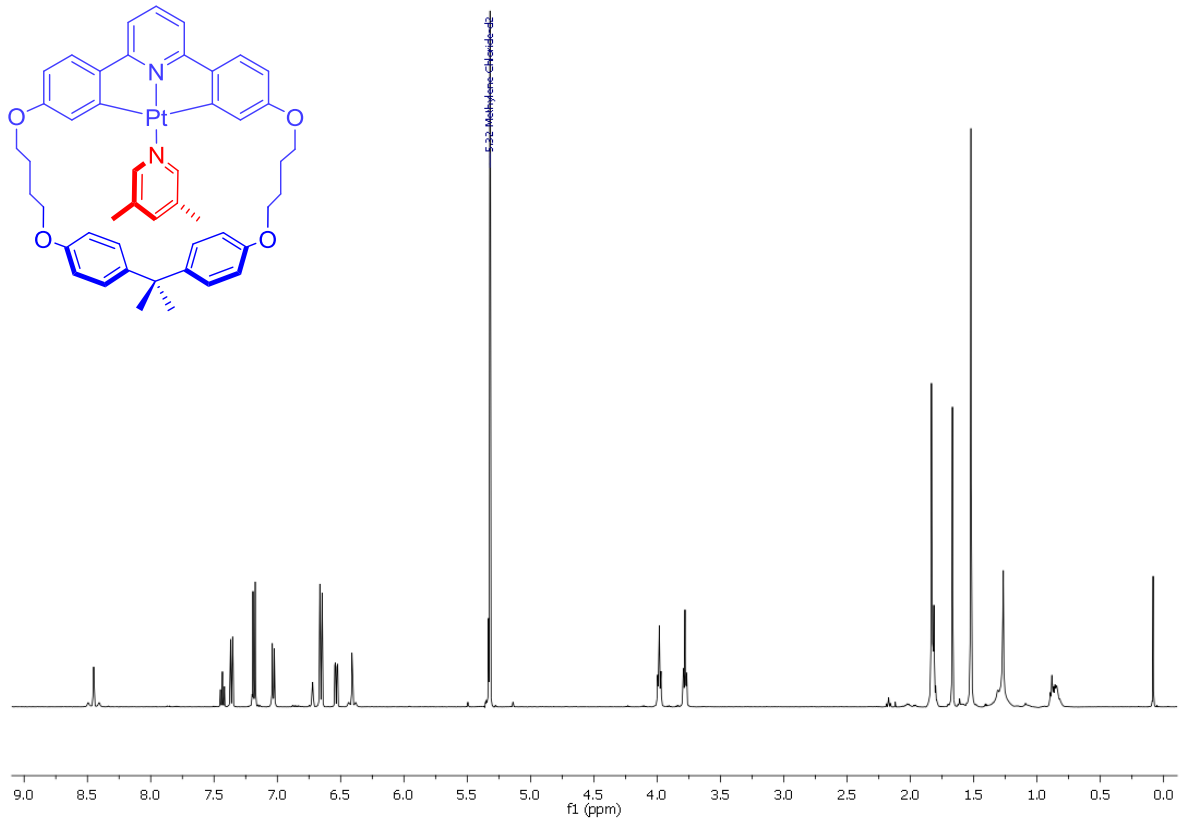

Figure S19. ^{1}H NMR spectrum (500 MHz, CD_2Cl_2, 298 K) of [$\mathbf{L^2}$Pt(3,5-Lut)].

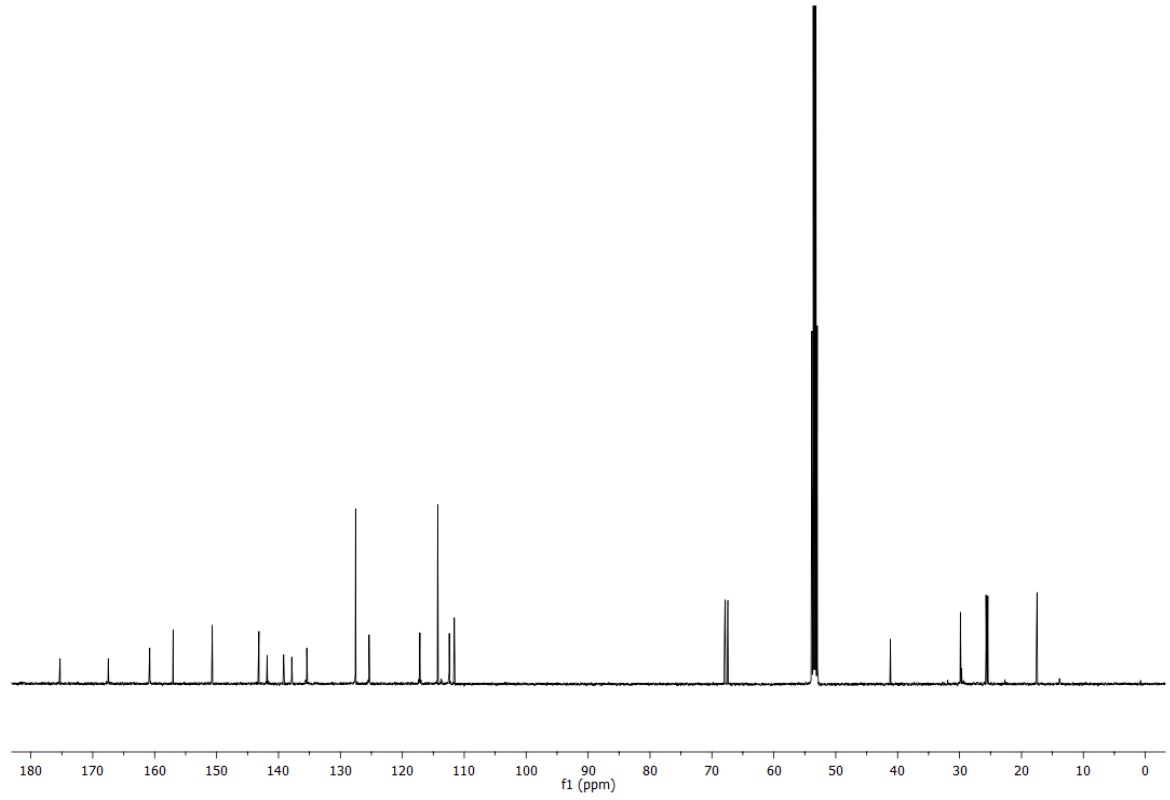

Figure S20. ^{13}C NMR spectrum (125 MHz, CD_2Cl_2, 298 K) of [$\mathbf{L^2}$Pt(3,5-Lut)].

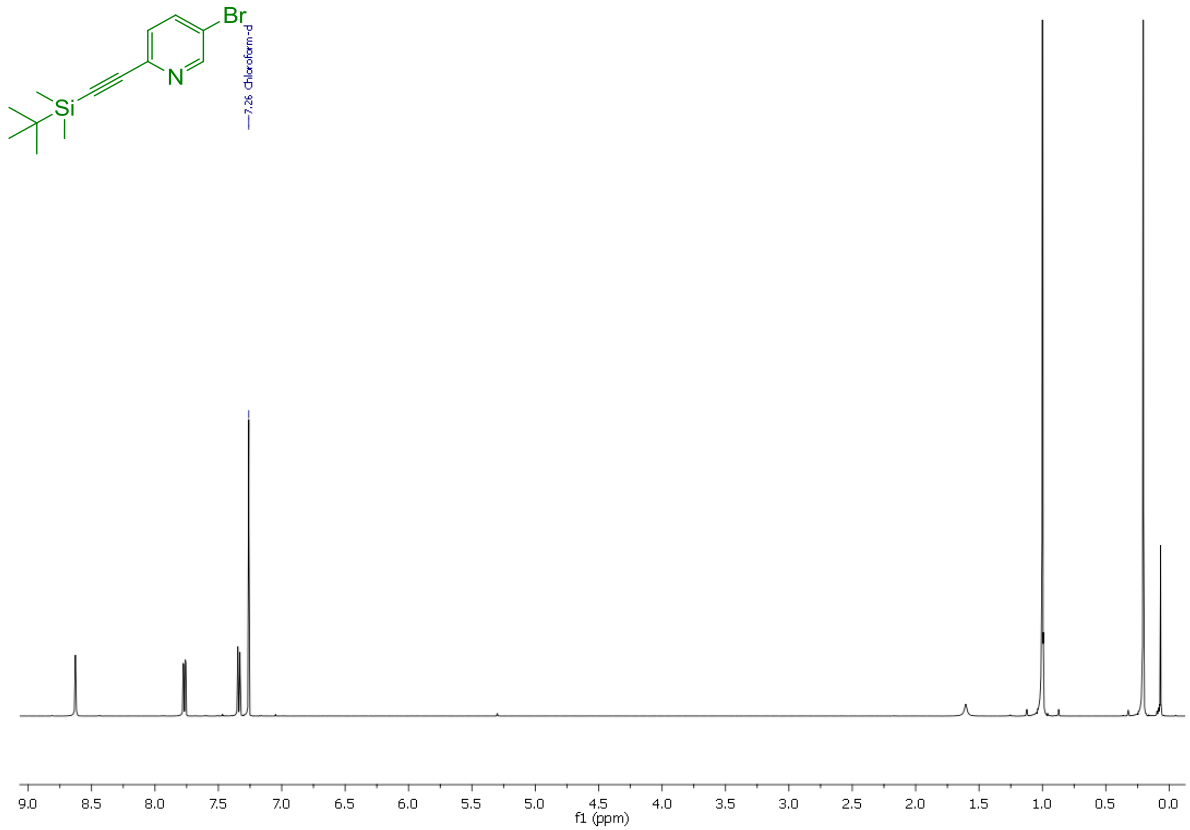

Figure S21. ^{1}H NMR spectrum (500 MHz, $CDCl_3$, 298 K) of 2-*tert*-butyldimethylsilylethynyl-5-bromopyridine.

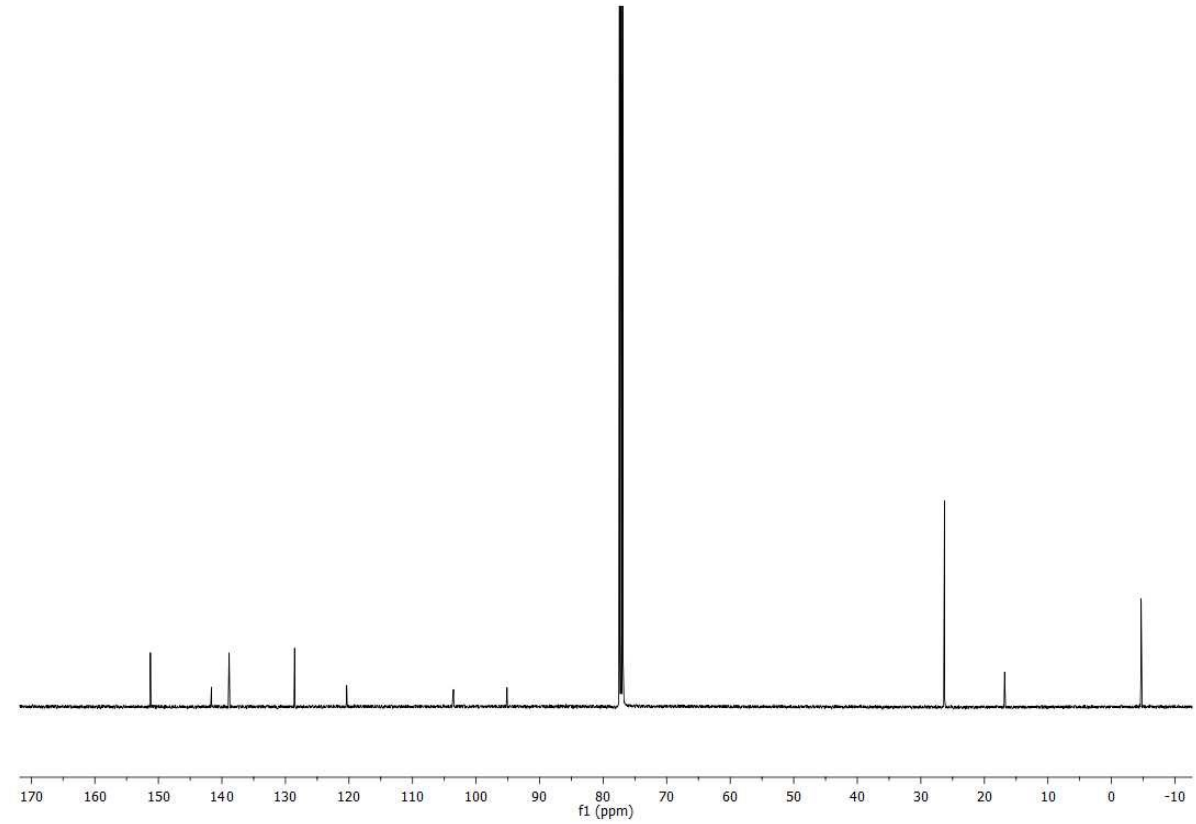

Figure S22. ^{13}C NMR spectrum (125 MHz, $CDCl_3$, 298 K) of 2-*tert*-butyldimethylsilylethynyl-5-bromopyridine.

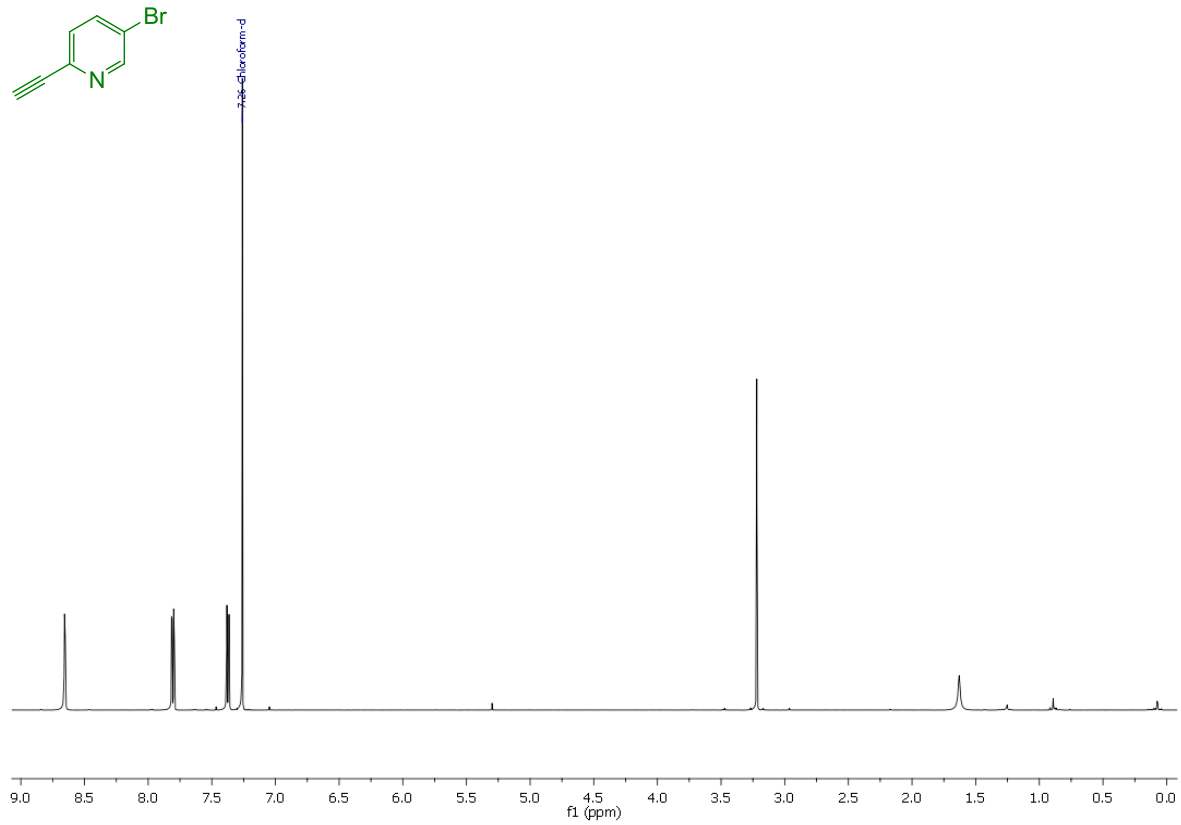

Figure S23. ^{1}H NMR spectrum (500 MHz, $CDCl_3$, 298 K) of 2-ethynyl-5-bromopyridine.

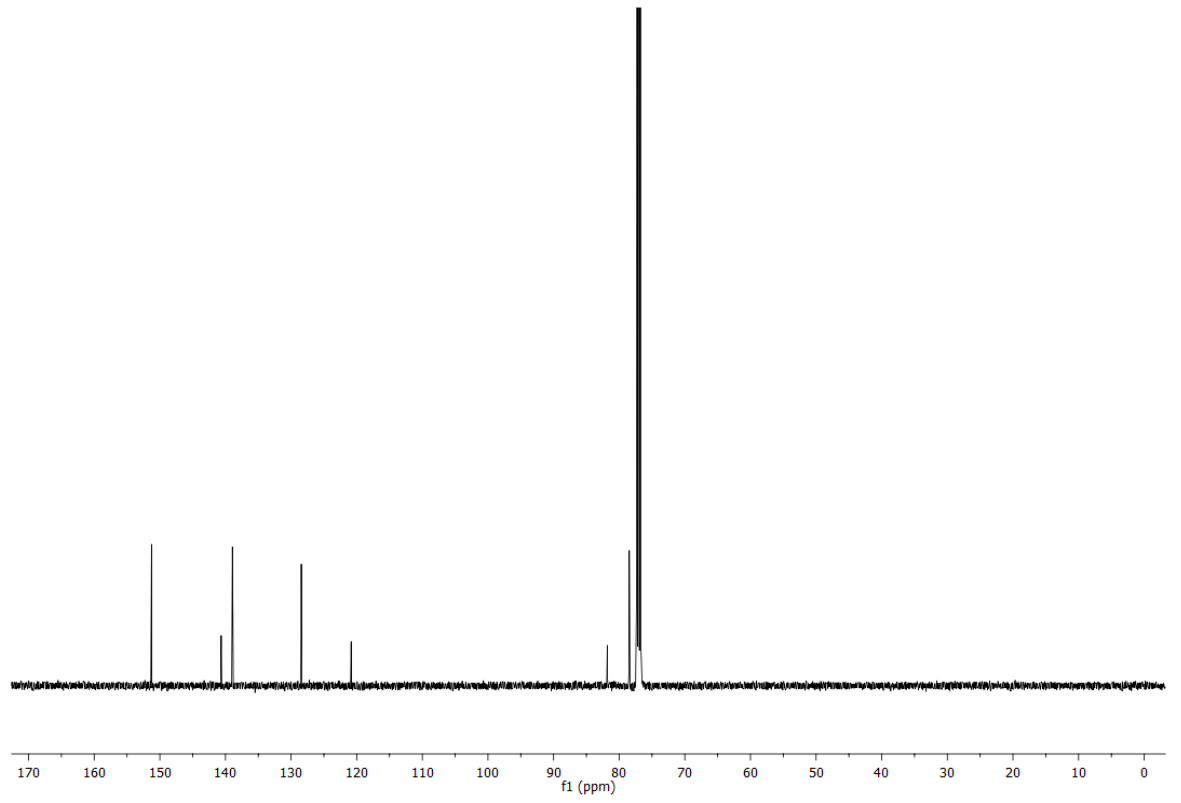

Figure S24. ^{13}C NMR spectrum (125 MHz, $CDCl_3$, 298 K) of 2-ethynyl-5-bromopyridine.

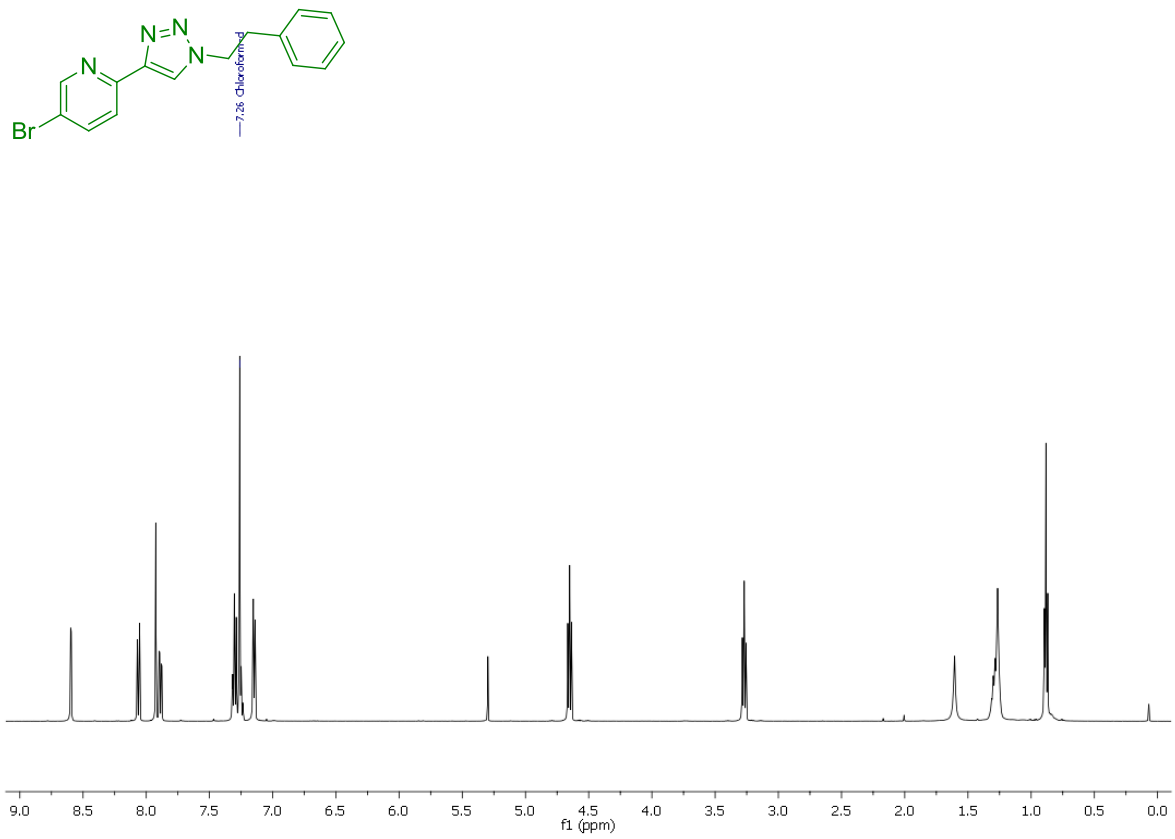

Figure S25. ^{1}H NMR spectrum (500 MHz, $CDCl_3$, 298 K) of $\mathbf{L^3}$.

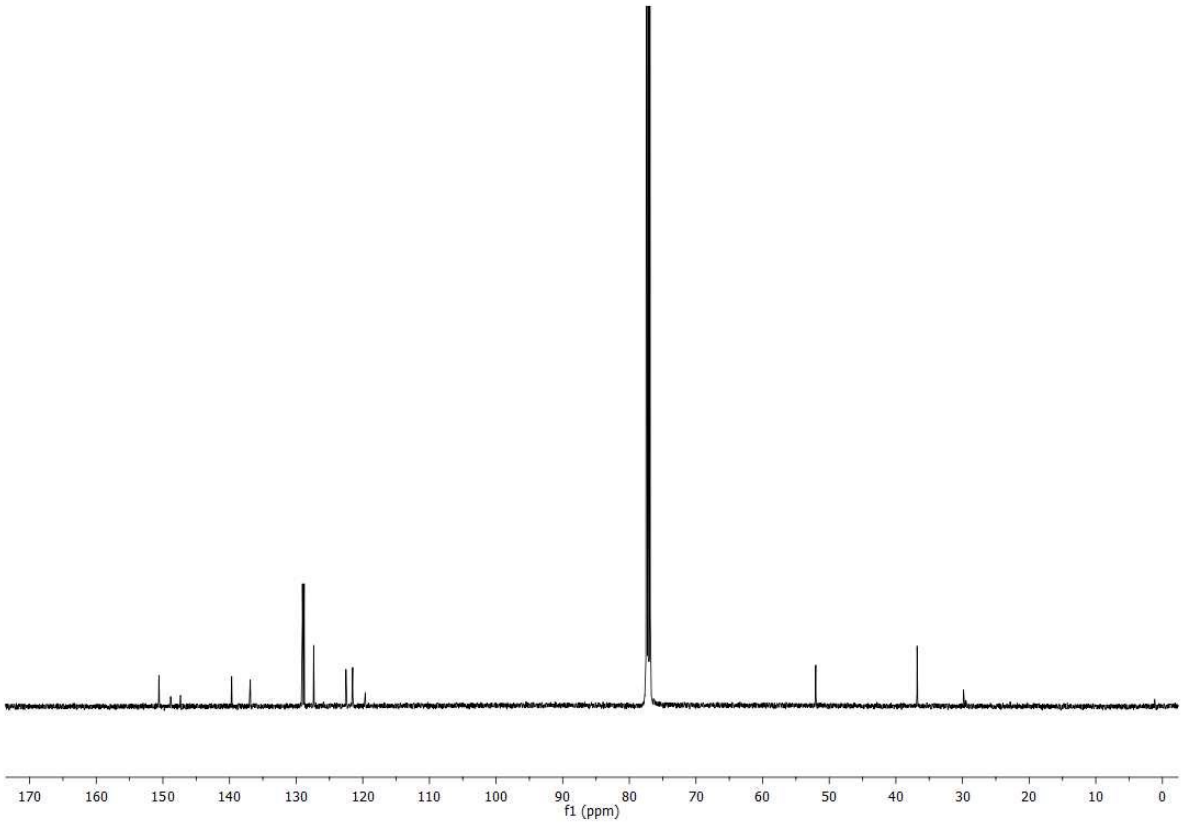

Figure S26. ^{13}C NMR spectrum (125 MHz, $CDCl_3$, 298 K) of $\mathbf{L^3}$.

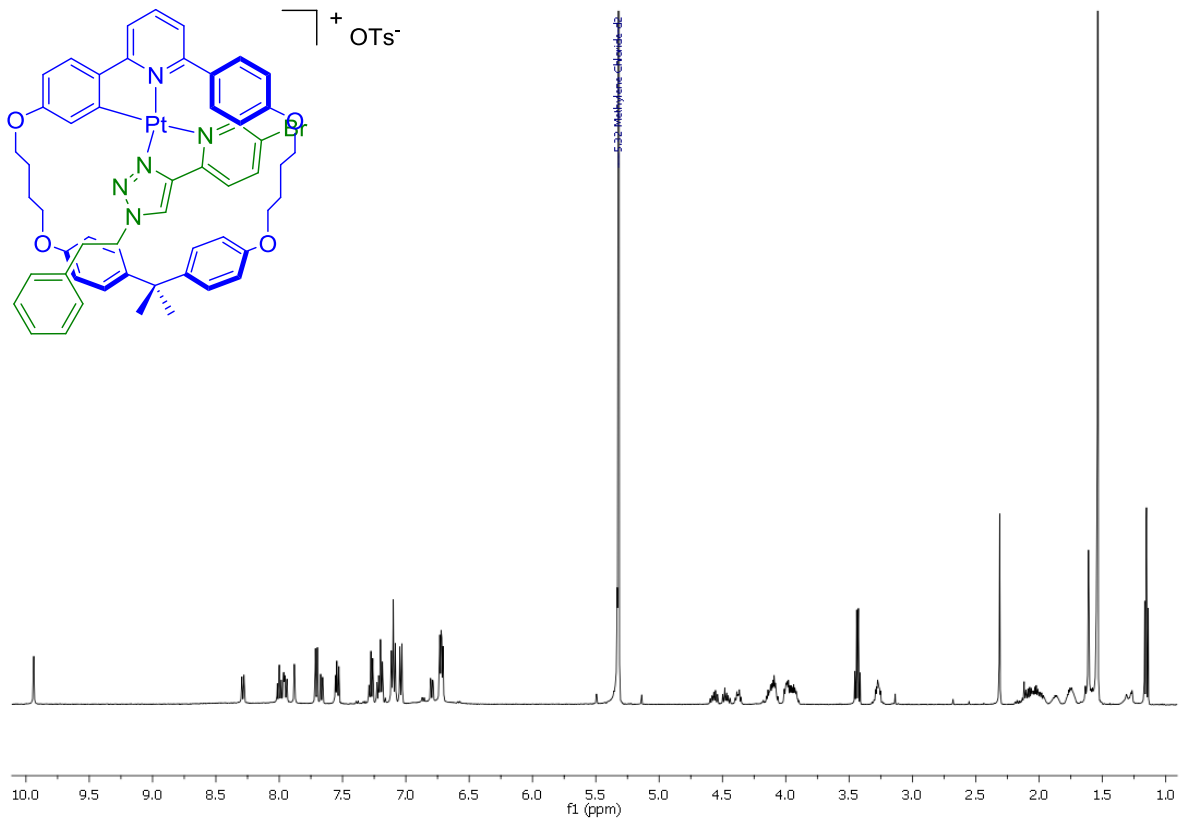

Figure S27. ^{1}H NMR spectrum (500 MHz, CD_2Cl_2, 298 K) of [$\mathbf{L}^2$Pt($\mathbf{L}^3$)]OTs.

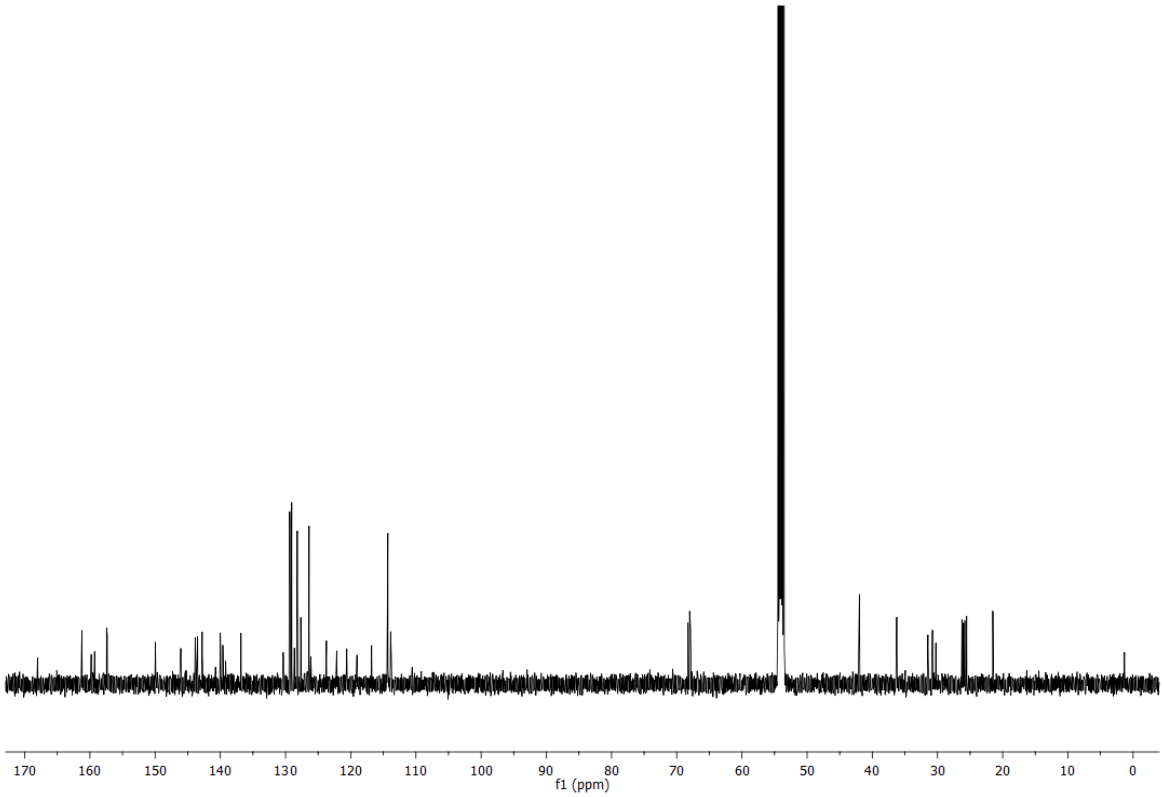

Figure S28. ^{13}C NMR spectrum (125 MHz, CD_2Cl_2, 298 K) of [$\mathbf{L}^2$Pt($\mathbf{L}^3$)]OTs.

1H-1H NOESY spectra of [HL^{1}Pt(dmbipy)]OTs and *trans*-[L^{2}Pt(L^3)]OTs and justification for absolute assignment of *trans*-[L^{2}Pt(L^3)]OTs

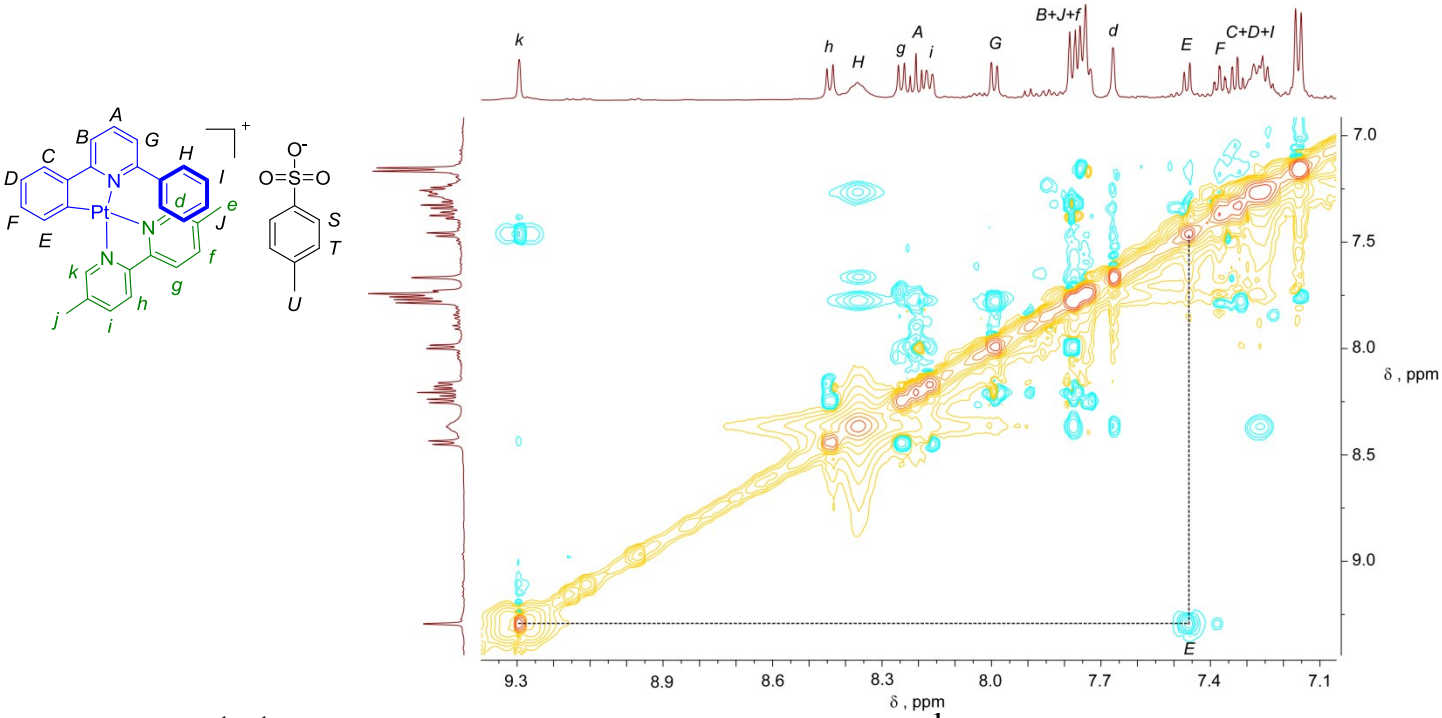

Figure S29. ^{1}H-^{1}H NOESY spectrum (500 MHz, CD_2Cl_2, 298 K) of [H**L**^{1}Pt(dmbipy)]OTs.

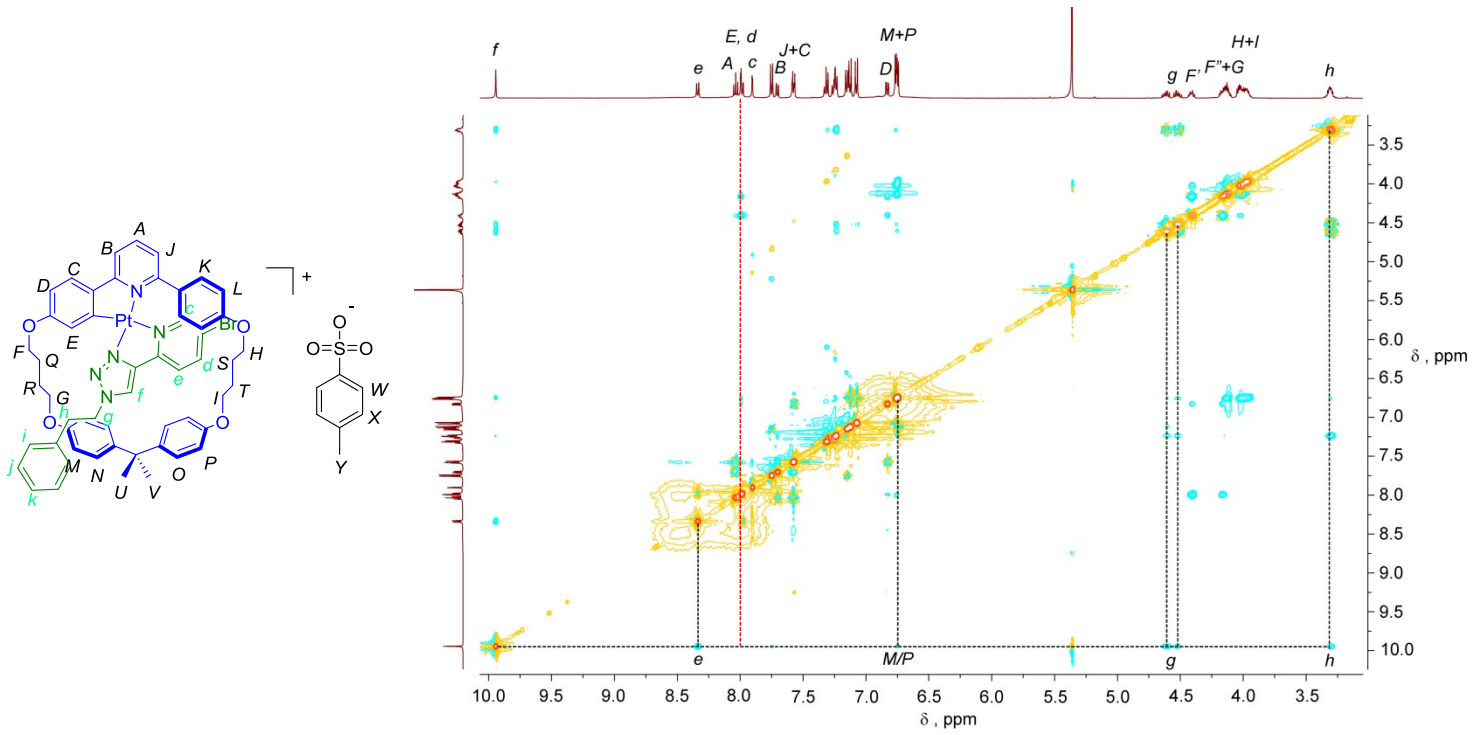

Figure S30. ^{1}H-^{1}H NOESY spectrum (500 MHz, CD_2Cl_2, 298 K) of [**L**^{2}Pt(**L**^{3})]OTs.

The absolute assignment of *trans*-[**L**^{2}Pt(**L**^{3})]OTs is made on the basis of the following observations:

(i) The presence of a strong NOESY signal between H_E and H_k in the acyclic "2+2" complex, [H**L**^{1}Pt(dmbipy)]OTs (Figure S29) and a clear lack of corresponding cross-peak between the signal at just below 10 ppm with H_E for [H**L**^{2}Pt(**L**^{3})]OTs (Figure S30).

(ii) Clear NOESY cross peak between the resonance at just below 10 for [H**L**^{2}Pt(**L**^{3})]OTs (Figure S30) and signals which can be ascribed to H_e, H_g and H_h of the **L**^{3} ligand.

(iii) The relative chemical shifts of the H_c and H_f resonances – whereas H_f is deshielded with respect to the same signal for free **L**^{3} (due to Pt complexation), H_c is upfield shifted by ca. 05 ppm, a result of shielding by the non-coordinating phenoxy alkyl group of **L**^{2}.

Comparison of the ^{1}H NMR spectra of [H**L**^{1}Pt(dmbipy)]OTs, [H**L**^{1}Pt(dmbipy)]CSA **and** [H**L**^{1}Pt(dmbipy)]OTs + TRISPHAT

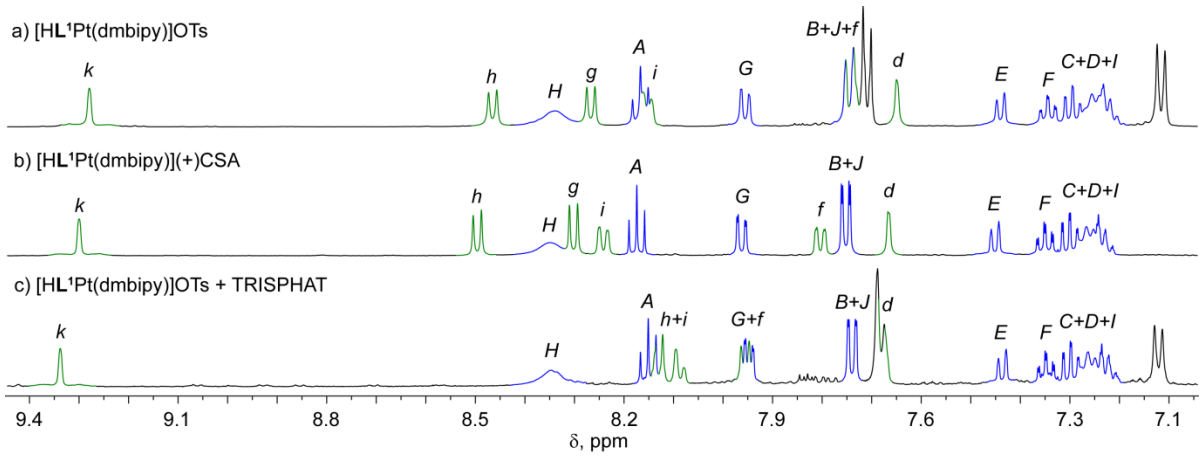

Figure S31. Partial ^{1}H NMR spectra (500 MHz, CD_2Cl_2, 298 K) of a) [H**L**^{1}Pt(dmbipy)]OTs, b) *in situ* generated [H**L**^{1}Pt(dmbipy)](+)CSA and c) [H**L**^{1}Pt(dmbipy)]OTs + TRISPHAT.

Reference:

[1] T. Bunlaksananusurn, K. Polburn, P. Knochel, *Angew. Chem. Int. Ed.*, 2003, **42**, 3941.

[2] (a) G. W. V. Cave, F. P. Fanizzi, R. J. Deeth, W. Errington, J. P. Rourke, *Organometallics*, 2000, **19**, 1355; (b) J. D. Crowley, I. M. Steele, B. Bosnich, *Inorg. Chem.*, 2005, **44**, 2989.

[3] S. J. Pike, P. J. Lusby, *Chem. Commun.*, 2010, **46**, 8338-8340.

[4] F. Durola, J. –P. Sauvage, O. S. Wenger, *Helv. Chim. Acta*., 2007, **90**, 1439-1446.

[5] G. Colombano, C. Travelli, U. Galli, A. Caldarelli, M.G. Chini, P. L. Canonico, G. Sorba, G. Bifulco, G. C. Tron, A. A. Genazzani, *J. Med. Chem.,* 2010, **53**, 616-623.

[6] V. Aucagne, J. Berná, J. D. Crowley, S. M. Goldup, K. D. Hänni, D. A. Leigh, P. J. Lusby, V. E. Ronaldson, A. M. Z. Slawin, A. Viterisi, D. B. Walker, *J. Am. Chem. Soc*. 2007, **129**, 11950-11963.